QEX

A Forum for Communications Experimenters

May / June 2023
Issue No. 338 | www.arrl.org

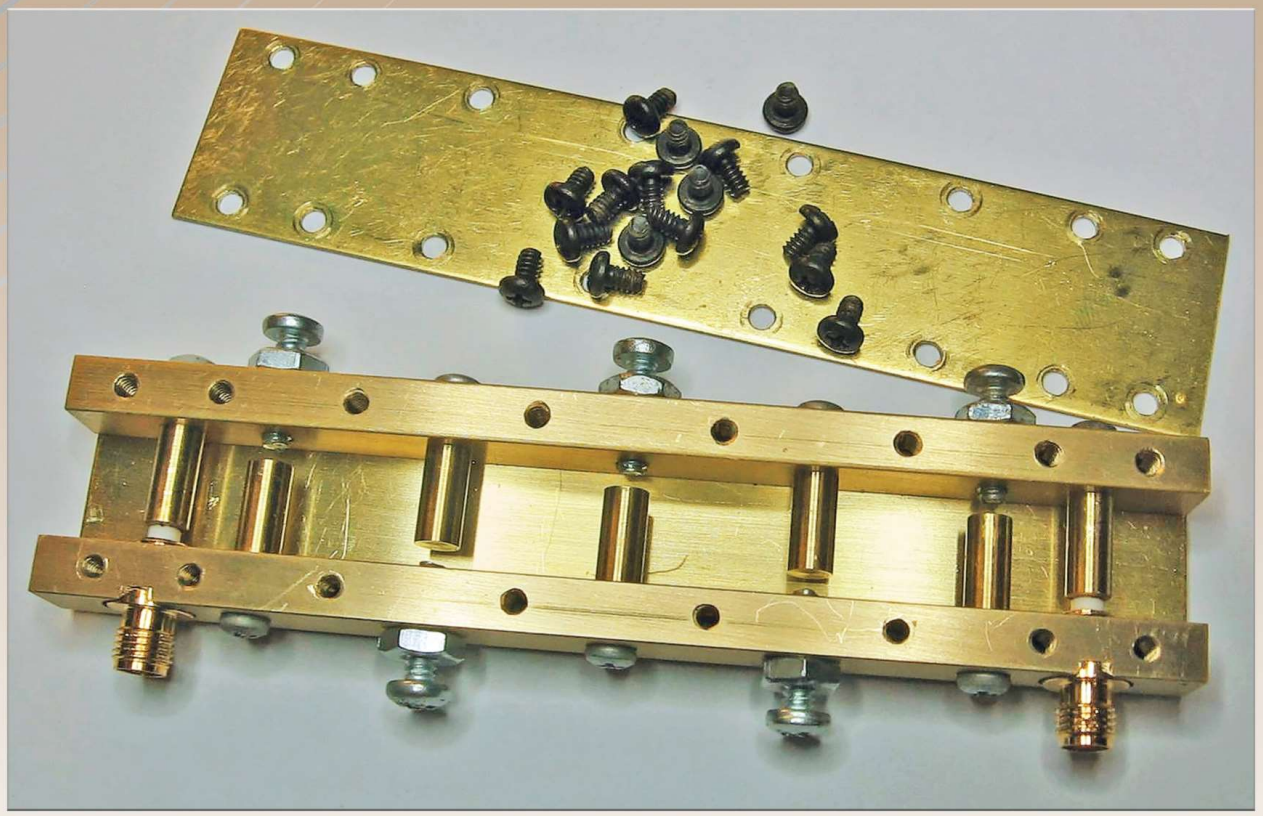

WA4LPR designs interdigitated filters using *INTRFIL*.

The EVENT HORIZON OF DX

TS-990S

Dual TFT Display & Dual Receiver HF/50 MHz Transceiver

The main receiver has an IP3 in the +40 dB class, and the sub receiver is the already famous TS-590S receiver. Capable of receiving two signals at once, on different bands. 7-inch and 3.5-inch color TFT displays allow displaying of independent contents. Simplification of complex operations at a glance. Make no mistake, this is not a toy. Finally a serious tool is available for getting the very most from your hobby, of course it's a Kenwood.

- Covers the HF and 50 MHz bands.
- High-speed automatic antenna tuner.
- USB, Serial and LAN ports.
- Various PC applications (free software): ARCP-990 enabling PC control, ARHP-990 enabling remote control, and ARUA-10 USB audio driver.
- Clean 5 to 200 W transmit power through the 50 V FET final unit.
- Built-in RTTY and PSK.
- Three Analog Devices 32-bit floating-point arithmetic DSPs.
- DVI output for display by an external monitor (main screen display only).

KENWOOD

Customer Support: (310) 639-4200
Fax: (310) 537-8235

www.kenwood.com/usa

ISO9001 Registered
Professional Systems Business Group
JVCKENWOOD Corporation

ADS#05421

QEX

QEX (ISSN: 0886-8093) is published bimonthly in January, March, May, July, September, and November by the American Radio Relay League, 225 Main St., Newington, CT 06111-1400. Periodicals postage paid at Hartford, CT and at additional mailing offices.

POSTMASTER: Send address changes to: QEX, 225 Main St., Newington, CT 06111-1400 Issue No. 338

Publisher
American Radio Relay League

Kazimierz "Kai" Siwiak, KE4PT
Editor

Lori Weinberg, KB1EIB
Assistant Editor

Ray Mack, W5IFS
Contributing Editors

Production Department
Becky R. Schoenfeld, W1BXY
Director of Publications and Editorial

Jodi Morin, KA1JPA
Assistant Production Supervisor

David Pingree, N1NAS
Senior Technical Illustrator

Brian Washing
Technical Illustrator

Advertising Information
Janet L. Rocco, W1JLR
Business Services
860-594-0203 – Direct
800-243-7768 – ARRL
860-594-4285 – Fax

Circulation Department
Cathy Stepina
QEX Circulation

Offices
225 Main St., Newington, CT 06111-1400 USA
Telephone: 860-594-0200
Fax: 860-594-0259 (24-hour direct line)
Email: **qex@arrl.org**

Subscription rate for 6 print issues:
In the US: $29

US by First Class Mail: $40

International and Canada by Airmail: $35

ARRL members receive the digital edition of *QEX* as a member benefit.

In order to ensure prompt delivery, we ask that you periodically check the address information on your mailing label. If you find any inaccuracies, please contact the Circulation Department immediately. Thank you for your assistance.

May/June 2023

About the Cover

Dennis Sweeney, WA4LPR, creates interdigitated bandpass filters with *INTRFIL* software. The design uses quarter-wavelength long round rods between parallel ground planes. Two test filters, one for 5760 MHz and the other for 2310 MHz, are designed, with simulated and measured results presented. Although the 5760 MHz filter had significantly higher loss than predicted, the agreement between design, simulation and measurement is encouraging. The 2310 MHz filter had an almost perfectly formed passband centered on 2359 MHz with no tuning. Precision is important but the results were encouraging enough that you could build a filter from the computer design and have confidence in its performance without sophisticated test equipment. *INTRFIL* should be useful in designing filters in the 500 to 6000 MHz range that will satisfy almost any amateur need.

In This Issue:

Index of Advertisers

The American Radio Relay League

The American Radio Relay League, Inc., is a noncommercial association of radio amateurs, organized for the promotion of interest in Amateur Radio communication and experimentation, for the establishment of networks to provide communications in the event of disasters or other emergencies, for the advancement of the radio art and of the public welfare, for the representation of the radio amateur in legislative matters, and for the maintenance of fraternalism and a high standard of conduct.

ARRL is an incorporated association without capital stock chartered under the laws of the state of Connecticut, and is an exempt organization under Section 501(c)(3) of the Internal Revenue Code of 1986. Its affairs are governed by a Board of Directors, whose voting members are elected every three years by the general membership. The officers are elected or appointed by the Directors. The League is noncommercial, and no one who could gain financially from the shaping of its affairs is eligible for membership on its Board.

"Of, by, and for the radio amateur," ARRL numbers within its ranks the vast majority of active amateurs in the nation and has a proud history of achievement as the standard-bearer in amateur affairs.

A *bona fide* interest in Amateur Radio is the only essential qualification of membership; an Amateur Radio license is not a prerequisite, although full voting membership is granted only to licensed amateurs in the US.

Membership inquiries and general correspondence should be addressed to the administrative headquarters:

ARRL
225 Main St.
Newington, CT 06111 USA
Telephone: 860-594-0200
FAX: 860-594-0259 (24-hour direct line)

Officers

President: Rick Roderick, K5UR
P.O. Box 1463, Little Rock, AR 72203

The purpose of *QEX* is to:

1) provide a medium for the exchange of ideas and information among Amateur Radio experimenters,

2) document advanced technical work in the Amateur Radio field, and

3) support efforts to advance the state of the Amateur Radio art.

All correspondence concerning *QEX* should be addressed to the American Radio Relay League, 225 Main St., Newington, CT 06111 USA. Envelopes containing manuscripts and letters for publication in *QEX* should be marked Editor, *QEX*.

Both theoretical and practical technical articles are welcomed. Manuscripts should be submitted in word-processor format, if possible. We can redraw any figures as long as their content is clear. Photos should be glossy, color or black-and-white prints of at least the size they are to appear in *QEX* or high-resolution digital images (300 dots per inch or higher at the printed size). Further information for authors can be found on the Web at **www.arrl.org/qex/** or by e-mail to **qex@arrl.org**.

Any opinions expressed in *QEX* are those of the authors, not necessarily those of the Editor or the League. While we strive to ensure all material is technically correct, authors are expected to defend their own assertions. Products mentioned are included for your information only; no endorsement is implied. Readers are cautioned to verify the availability of products before sending money to vendors.

Kazimierz "Kai" Siwiak, KE4PT

Perspectives

A Diverse Group

Let us pause here to examine what defines us, and to ask what is common among members of the following group of vocations and occupations:

Actor, Administrator, Ambassador, Artist, Astronaut, Author, Cosmonaut, Designer, Director, Engineer, Grade School Student, King, Lawyer, Manager, Musician, Nobel Laureate, Prime Minister, Prince, Professor, Programmer, Queen, Senator, Singer, Teacher, Technician, Tradesman, Writer.

The list is far from comprehensive; it is what hams of many walks of life have achieved, and what some hams do or did for a living. What binds us together is that each member of the group holds an amateur radio license. We hams are a diverse lot with a global span, and we range in age from pre-teen to centenarian. For many of us, our vocation does not match our avocation, so we bring varied perspectives to our hobby. Amateur radio brings our world together. Our diversity is our strength.

How has amateur radio influenced your life? How have you influenced amateur radio?

In This Issue:

- Wesley Cardone, N8QM, characterizes an accurate *SPICE* diode model.
- Dennis Sweeney, WA4LPR, simulates and designs interdigitated filters with *INTRFIL*.
- Russ Ward, W4NI, designs filters with *Octave*.
- John M. Franke, WA4WDL, repurposes waveguide sections to serve as drilling guides.
- H. Scott Lentz, AG7FF, designs a high image rejection receiver.
- Keith Stammers, GØSXG, derives a graphical solution to the parallel impedance problem.
- Dr. Philip Cassady, K7PEC, clarifies and improves tuned transformers.
- In his essay series, Eric P. Nichols, KL7AJ, discusses distributed circuits.

Writing for *QEX*

Please continue to send in full-length *QEX* articles, or share a **Technical Note** of several hundred words in length plus a figure or two. *QEX* is edited by Kazimierz "Kai" Siwiak, KE4PT, (**ksiwiak@arrl.org**) and is published bimonthly. *QEX* is a forum for the free exchange of ideas among communications experimenters. All members can access digital editions of all four ARRL magazines: *QST*, *OTA*, *QEX*, and *NCJ* as a member benefit. The *QEX printed edition* is available at an annual subscription rate (6 issues per year) for members and non-members, see **www.arrl.org/qex**.

Would you like to write for *QEX*? We pay $50 per published page for full articles and *QEX* Technical Notes. Get more information and an Author Guide at **www.arrl.org/qex-author-guide**. If you prefer postal mail, send a business-size self-addressed, stamped (US postage) envelope to: *QEX* Author Guide, c/o Maty Weinberg, ARRL, 225 Main St., Newington, CT 06111.

Very kindest regards,
Kazimierz "Kai" Siwiak, KE4PT
QEX Editor

Wesley Cardone, N8QM
10626 Coopersfield Rd., Chelsea, MI 48118 | **n8qm@arrl.net**

Precision Generic Diode Characterization for Simulation

Solving for the SPICE diode dc characterization parameters facilitates a duplication of published performance.

The characterization of a Simulation Program with Integrated Circuit Emphasis (SPICE) diode can have high fidelity reproducing, in computer simulation, its published current-voltage (IV) profile for its reference ambient temperature. However, a loss of fidelity will be observed with ambient temperatures differing from the reference temperature (TNOM). Therefore, industry-released device-specific model characterizations are designed to satisfy a wide range of ambient temperatures by uniformly distributing the error. This paper will explain the nature of the SPICE diode model and how to solve for its dc characterization parameters given a published reference ambient temperature profile. A simulation diode model so characterized will virtually superimpose itself over the published IV profile for the reference ambient temperature.

Background

SPICE was originally developed by the University of California, Berkley as a class project in 1969-70 and was released into the public domain in 1972 as Version 1. In 1975 version 2g.6 was released, which became the backbone of analog circuit computer simulation on a global scale though only available by mainframe.

With the release of the Intel 80486 processor in 1980, with its 32-bit architecture, personal computers became powerful enough to accommodate SPICE without special AT bus boards. Many companies embedded public domain SPICE 2g.6 within their own graphical user interfaces selling the software as a sophisticated analog circuit simulation tool. But while SPICE 2g.6 was quite sophisticated in its numerical processing for analog design, characterizations for discreet analog components such as bipolar junction transistors and diodes were virtually non-existent. There were a number of companies that developed SPICE libraries for sale at very high prices. High prices, of course, effectively made them unavailable for hobbyists and companies on limited budgets.

In 1999, Linear Technology released its first version of LTSpice, which is free software originally developed by Linear Technology. An LTSpice download may be obtained at the **www.analog.com** website. Upon entry to that website, enter the search terms "ltspice download" for Microsoft Windows. The current release of LTSpice (17.1) has had many enhancements and new capabilities together with a very extensive professional library of discrete semi-conductor components. Virtually all of today's desktop and laptop computers (Mac and Windows) are capable of running LTSpice. The sophistication of SPICE for the hobbyist has arrived.

The Spice Diode Model

The diode model found in LTSpice, though it has many enhancements relative to SPICE 2g.6, still includes the original functionality of the SPICE diode model. In the following text we will first look at what physical performance to expect from a silicon diode under controlled environmental conditions and then compare those with the SPICE diode simulation model.

Figure 1 depicts the fundamental dc functionality for the physical silicon diode's current-voltage (IV) profile. The curve represents measurements taken for this paper using a 1N914 diode immersed in a 0 °C water bath. For a given diode forward voltage (linear Y-axis) there is a dependent current (log X-axis). There are two regions of interest for simulation and design purposes described below. In **Figure 1**, the wavy curve illustrates the physical IV performance for the physical 1N914 silicon diode through all its regions at 0 °C. There are two regions of interest for both practical design and therefore simulation: ideal and resistive. Note that the physical curve departs from either of the two straight lines at two places. The departure that occurs for forward voltages less than 0.6 V is not directly accounted for by the SPICE diode model and neither is it of interest for practical design purposes. However, this region of operation (with its very low forward voltages) is roughly

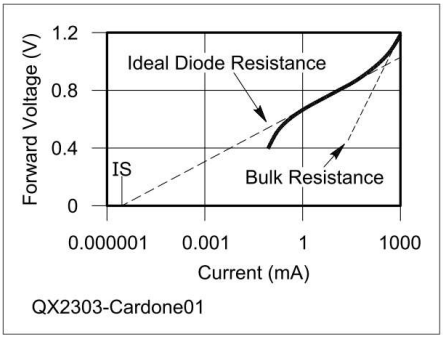

Figure 1 — Illustration of the physical nature of the silicon diode with reference to its regions of operation: recombination; ideal; and high injection. The data of this figure were taken with the device under test immersed in an ice water bath.

accounted for by means of the *GMIN* (minimum conductance) parameter described later in this paper.

SPICE uses the Shockley diode equation to solve for a forward voltage given a current and ambient temperature:

$$V_f = N V_t \log_e \left\{ \frac{i}{IS} + 1 \right\} + i\,RS + V_f GMIN$$

William Shockley of Bell Telephone Laboratories developed the IV (current-voltage) characteristic equation representing an idealized diode for either forward or reverse bias applications.

Within this equation there are three foundational parameters governing a diode's dc performance — *N* (emission coefficient), *IS* (saturation current), and *RS* (bulk resistance). A thermal voltage, V_t, is a function of the environment and cannot be manipulated by the user. There is a minimal conductance, *GMIN*, that governs the diode at very low forward voltages, V_f. Here the product (V_f *GMIN*) will begin to dominate the above equation.

The most significant region in **Figure 1** is the ideal. Here, the diode's PN junction follows a semi-log path as a function of the forward voltage. The "ideal diode region" line covers the device ideal mode operation but for illustration purposes extrapolates into the adjacent regions. Observe the intercept point where the ideal curve extrapolation crosses zero volts. The corresponding current represents the diode's saturation current and is marked in **Figure 1** by the solid wavy line. The simulation would return an *IS* current for a zero voltage drop except for the minimal conductance parameter, *GMIN*. All device models in SPICE have a *GMIN* parameter to circumvent numerical convergence issues associated with zero.

Crucial to understanding the premise of this paper, the saturation current *IS* has a dependence on the ambient temperature. As the ambient temperature increases, the saturation current also increases, given a forward voltage. In addition, as the ambient temperature increases, the emission coefficient (*N*) changes slightly. The sole purpose of the *XTI* parameter (in conjunction with *N*) is to move *IS* to make it track the ambient temperature. In practice, little change results from *XTI*. It is recommended to leave *XTI* at its default.

The important observation is that the SPICE diode model moves the curve in the correct direction to track a changing ambient temperature. However, the accurate quantification of that change is only rudimentary with respect to published profiles leaving much to be desired. This accounts for a need to characterize a given device for a best approximation where a wide range of ambient temperatures is to be allowed for.

Viewing **Figure 1**, consider the region where resistive effects are dominant (bulk resistance line). The SPICE diode model accounts for this region with a linear bulk resistance as illustrated graphically in **Figure 2**, dominant resistance line given by:

$$RS = \frac{V_f - V_{ext}}{i_d}$$

The bulk resistance (illustrated in **Figure 2**) serves as supplemental voltage drop to the ideal drop. At relatively low currents, the bulk resistance drop is not significant relative to the ideal drop. However, as current increases further, the voltage drop from the resistance begins to become measurable as a supplement to the diode ideal drop. At this point there are two voltage drops being summed together. Both drops continue to increase with increasing current though the resistive drop will eclipse the ideal drop with further increases in current.

The key to understanding how the SPICE diode model's bulk resistance parameter is developed, is graphically shown in **Figure 2**.

A pseudo data-pair may be picked at any point along the ideal mode straight-line extrapolation (V_{ext}, i_d). For this illustration, a point was picked at the crossing of the two straight lines for convenience. The current at this location also approximates a reasonable value for the *IKF* parameter, which is beyond the scope of this paper. Note that *IKF* is generally of little use and necessitates a change in *RS*.

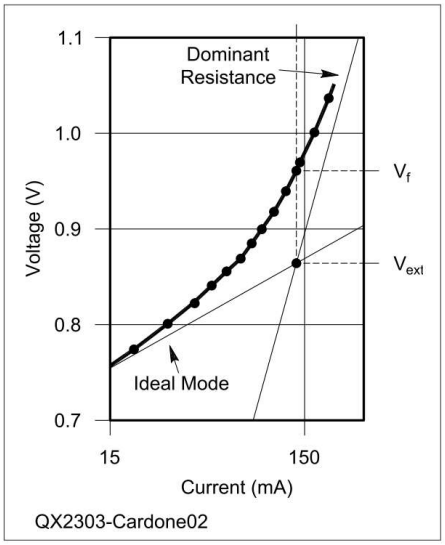

Figure 2 — Graphic illustration on obtaining the bulk resistance from the published IV profile.

A corresponding data pair having the same current is then identified on the device IV profile (V_d, i_d) curve with dots. The voltage difference between the actual device, V_f, and the extrapolated resistive drop, V_{ext}, divided by the common current, i_d, represents the resistance, *RS* given earlier.

While the pseudo data-pair may be selected from any point on the gray line, the data pair is best selected where the current is highest.

Solving for *RS* in this manner is unnecessarily complicated but serves as an excellent graphic illustration. A step-by-step equation set is given in the **Appendix** (see **Table 4**) to solve for the parameters *IS*, *N*, and *RS*. The **Table 4** simplified equations were derived from the above-described process.

What's The Difference?

We have noted that while the SPICE diode at least pushes the simulation IV curves in the correct direction with respect to a defined ambient temperature, it is not able to provide a high level of fidelity for a broad sweep of ambient temperatures. To demonstrate this, we will compare the Linear Technology Corporation's 1N914A released SPICE characterization with its published curves:

1N914 D(Is=2.52n Rs=0.568 N=1.752)

Referring to **Figure 3**, observe the heavy black lines showing the published outer limit ambient temperature values –40 °C +65 °C. These are relative to the nominal 25 °C, which has been shadowed out for simplicity. **Table 1** lists a comparison of published with simulation results for the three ambient temperatures, each at two or three forward voltages. The simulation results from **Table 1** are illustrated in **Figure 3** as heavy dots.

Observe in **Figure 3** that the simulation results (heavy dots) for –40 °C show a crossover point. With a forward voltage of 0.65 V the simulation returns 150 mA, which is the precision we can be satisfied with. But for the same temperature at any other forward voltage, the simulation

Table 1 – Simulation results using the LTSpice released characterization for the 1N914 diode. These six data-pair values (V_{fwd}, i_{fwd}) are shown graphically in Figure 3.

V_{fwd} (V)	T_{amb} (°C)	I_{fwd} (mA) Simulation	I_{fwd} (mA) Published
0.35	65	0.046	0.018
0.55	–40	0.0087	0.017
0.55	25	0.426	0.65
0.55	65	2.3	0.65
0.65	–40	150	150
0.65	25	3.76	1.9
0.65	65	14.0	3.9
0.75	–40	2.5	2.3

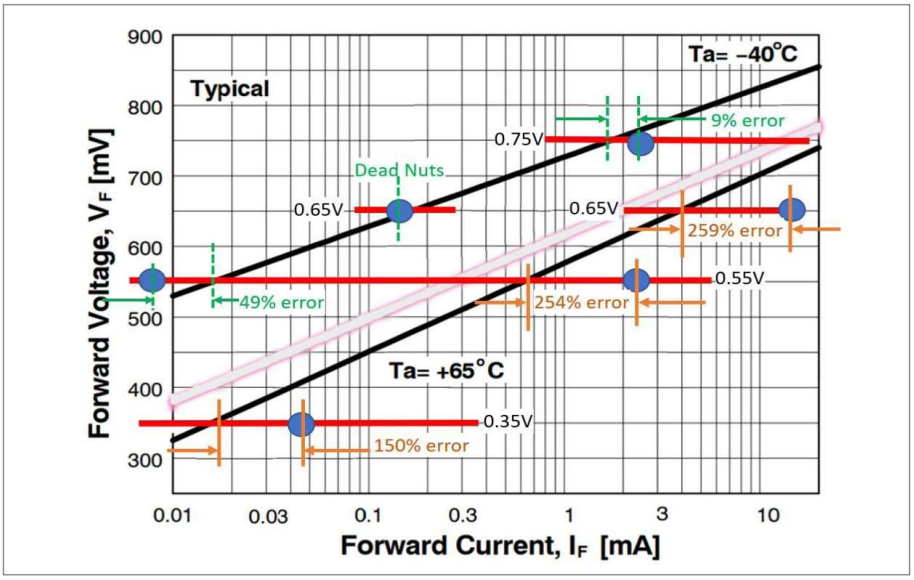

Figure 3 — Comparison of the published 1N914 IV performance curves (bold sloping lines) for named ambient temperatures together with selected simulation data-pair results from Table 1. The shadowed-out line de-emphasizes 25 °C for simplicity. The dots mark the data-pairs for returns of the SPICE simulation for the two ambient temperatures at forward voltages of 0.35, 0.55, 0.65, and 0.75 V.

returns results either too low or too high with errors less than 50%.

Moving to the simulation results at 65 °C we see that for the range plotted, all the returned currents are too high with errors greater than 150%. Though not illustrated, errors at 25 °C for the range plotted are from 35 to 98%.

This "even distribution" of error makes it clear that Linear Technology's characterization was intended to accommodate a logical best approximation across a wide-ranging set of ambient temperatures. It could be said that "nobody is right, but everybody is at least pretty close."

What is critical to note, however, is that the SPICE diode model has the capability to reproduce a published IV profile very accurately for a reference ambient temperature, whatever that may be. The premise of this paper centers around that critical observation.

Relevant Data Collection

Please refer to **Figure 4** illustrating that there are two processes that are operational simultaneously. One process is dominant under low current conditions and the other process is dominant under high current conditions. In addition, there is sharing in a transition region where the two meet. The raw data from **Figure 4** is assembled in

Table 2 – SPICE diode IS and N parameters for characterization at 25 °C (298.15 K) to replace those found within the LTSpice released model.

Temp (°C, K)	25, 298.15
N, emission coefficient	1.9807084
IS (nA) saturation current	5.5276707
RS (Ω) bulk resistance	0.6163538

Table 3 – The critical data from the published charts (see Figure 4) for solving for the characterization parameters shown in Table 2.

Data pair	V_f (V)	i_f (mA)
1	0.381682	0.01000
2	0.616516	1.00971
3	1.420452	757.7306

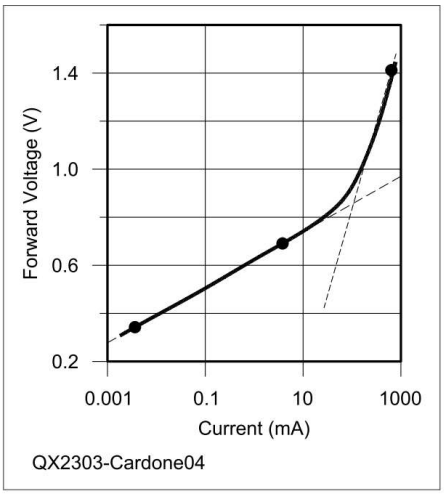

Figure 4 — The illustration depicts the foundation of characterization though data selection. The two straight lines depict the two relevant regions of operation: ideal (a function of the ideal diode equation) and resistive. The lowest current data pair must be selected low enough in voltage to not have any significant resistive influence.

Table 3 where the three data-pairs (V_f, i_f) upper, mid and lower dots, have been captured. The data pairs were then plugged into the solution protocol given in **Table 4** of the **Appendix**) to arrive at the solution set given in **Table 2**. This characterization will return very accurate results for transient analysis simulations where ambient temperatures are near 25 °C.

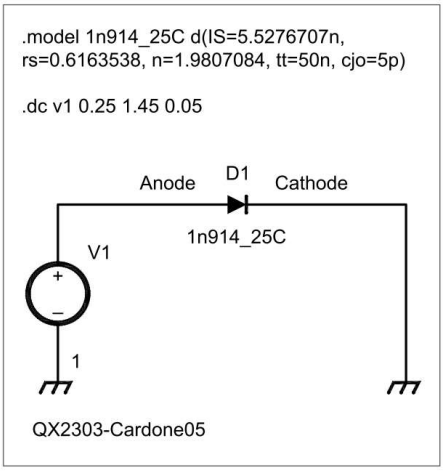

Figure 5 — LTSpice simulation circuit used to sweep the 1N914 diode from 0.25 V to 1.45 V in increments of 0.05 V. TT and CJO were given values even though they do not contribute to a dc solution. This is simply a good practice contributing to preventing convergence issues.

Deployment Characterization Example for the 1N914 Diode

Shown in **Figure 5** is a screen-capture from an LTSpice simulation to document the custom characterization (see **Table 2**) dc performance at the ambient temperature for which it was characterized: +25 ºC.

Note that two temporal parameters were included which do not affect dc performance — TT (transit time) and CJ0 (zero bias junction capacitance). If not specified, their values default to zero creating a remote possibility for a loss of numerical convergence.

Under some conditions where a design has switching functionality using a device without temporal understanding, SPICE may fail to converge due to what it detects as a discontinuity. That is, a signal that is supposed to be both one value and another value at the same time.

As humans, we look at a square wave and think "step-function." But we all know that buried deep within any oscilloscope square wave trace that there is a rise time. It is a good practice to include temporal parasitic model effects even when their presence is not going to be significant. The reason is that SPICE cannot understand a signal transition that takes place in zero time. When it encounters a discontinuity, it may possibly fail to converge aborting the simulation abnormally leaving you in the dark as to why.

Comparison of Custom With Released Characterization

In **Figure 6** there is a comparison of the LTSpice 1N914 diode with the custom characterization accomplished in this paper for an ambient temperature of 25 ºC.

It is important to note that this characterization was algorithmic, leaving very little to engineering judgment. The steps were to first identify three data pairs on the published curve for the ambient temperature of interest. We then plugged those data pairs into the equation solution mechanism found in **Table 4**. Three parameters were solved for: *N*, *IS*, and *RS*. With just these three parameters the characterization nearly superimposed itself over the published curve for the named ambient temperature with no iteration required for parameter values. Some might call this plug-and-chug.

But My Customization Didn't Superimpose

For the case where simulation results for a custom diode characterization produce excess error, consider choosing different data pairs from the published IV profile. The most common error is selecting data pair number 2 (reference **Table 3**) at too high of a current level where resistive effects are beginning to become significant.

Temperature within Transient Analyses

What makes the characterization process described in this paper of special relevance is that any specific diode characterization (becoming a library entry) will be for an explicitly named ambient temperature. For transient analyses at that ambient temperature, simulation results will track the published performance with extreme accuracy. When used in simulations where other ambient temperatures are specified, the model will make appropriate directional shifts but only in a rudimentary fashion. For those cases, it is recommended to use the LTSpice library characterization.

Most transient analyses are run at the default 27 °C ambient temperature where the LTSpice library characterizations will be only best-fit compromises. If high accuracy is required at (for example) -40 °C, it is recommended to characterize a device explicitly for -40 °C.

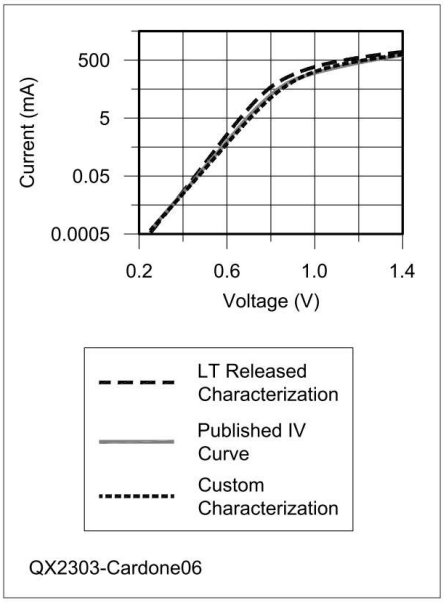

Figure 6 — Comparison of published performance with the simulation results (IS=5.5277 nA, N=1.9807, and RS=0.6163 Ω) for an ambient temperature of 25 °C.

Table 4 – Equations used to solve for the varied components of the overall characterization process. Temperature is in Kelvins.

Parameter	value
Thermal voltage	$V_t = kT/q$
k, J/K	1.3806E – 23
q, C	1.6022E – 19
Emission coefficient	$N = \frac{V_2 - V_1}{V_t ln\left(i_2 / i_1\right)}$
Saturation current	$IS = \frac{i_{1\ or\ 2}}{e^{V_{1\ or\ 2}/NV_t} - 1}$
Bulk resistance	$RS = \frac{V_3 - V_t N\ ln\left(i_3/IS\right)}{i_3}$

Conclusion

In most cases, the LTSpice distributed-error released model will be sufficient in supplying reasonably accurate results for any ambient temperature. However, it may also be that the forward characteristics with respect to the ambient temperature are critical such as in applications where the natural log characteristic of the silicon diode is used to accurately detect and quantify temperature changes within an electronic or other device.

It may also be that the diode called for in a design is not found in the LTSpice released library. A custom diode SPICE model characterization would be required. An example of a diode not found in the LTSpice library at the time of this writing is the 1N4729 Zener diode. Pick a temporally close proximity Zener characterization from the LTSpice library and substitute the *IS*, *N*, and *RS* parameters solved for here.

What we have shown in this paper is that the SPICE model diode is capable of accurate characterization for a published IV profile (for a named ambient temperature) for virtually all silicon diodes.

Appendix

The equations for the SPICE diode parameter characterizations are shown in **Table 4**. This is a step-by-step process that must be accomplished in order. Attempting to skip a step will immediately reveal the necessity of following an order since each step develops a variable that is used in the next step.

Refer to **Figure 4** as an aid in following the data-pair descriptions below. Data pair number 1 is taken at the lowest published current available. Data pair number 2 can be tricky to evaluate and correctly select. This data pair must be taken from the ideal region of operation with care taken to be certain that resistive effects are not significant. Data pair number 3 is readily identified as simply the data-pair with the highest current.

Wesley Cardone , N8QM, graduated from Cal Poly, San Luis Obispo with a BSEE. He has worked for Boeing at both Vandenburg AFB and Seattle, and the Johns Hopkins University Applied Physics Laboratory in Maryland. He has also worked in the automotive industry for Ford Motor, Lear Corporation, Fiat-Chrysler, and Caresoft Global of Livonia. Wes has pursued amateur radio since 2018 and currently serves as trustee for the Chelsea Amateur Radio Club (CARC) repeater. Wes also teaches a weekly class by video conference in amateur radio electromagnetics, sponsored by CARC. The class is designed for the licensed amateur radio public not highly schooled in electronics but wanting to upgrade to the amateur radio General and Amateur Extra classes. The class is named, "I Hate Cookbooks Guide to Amateur Radio Electromagnetics." It is premised upon the concept that we can become creative when we understand the gut-level simple underlying principles behind what moves RF technology.

Dennis Sweeney, WA4LPR
1206 Westover Dr., Blacksburg, VA 24060 | **dsweeney@vt.edu**

Design and Construction of Round Rod Interdigitated Filters

Simulate and design interdigitated filters with *INTRFIL*.

This paper describes *INTRFIL*, a program intended to create band-pass filters using interdigitated round rod ¼ wavelength long resonators between parallel ground planes (slab line), see **Figure 1** for an example of a filter designed to have an approximately 35 MHz (3 dB points) bandwidth centered at 5760 MHz. The lid is 1.00 inch wide. There are 7 rods. The rods at the far ends of the filter are not resonators but coupling rods.

A simulation technique synthesized from pairs of coupled lines in the open source circuit simulator *QUCS* (Quite Universal Circuit Simulator) **[1]** is described. This simulation technique is useful for verifying a design. Test filters for 2304 MHz and 5760 MHz are included as examples.

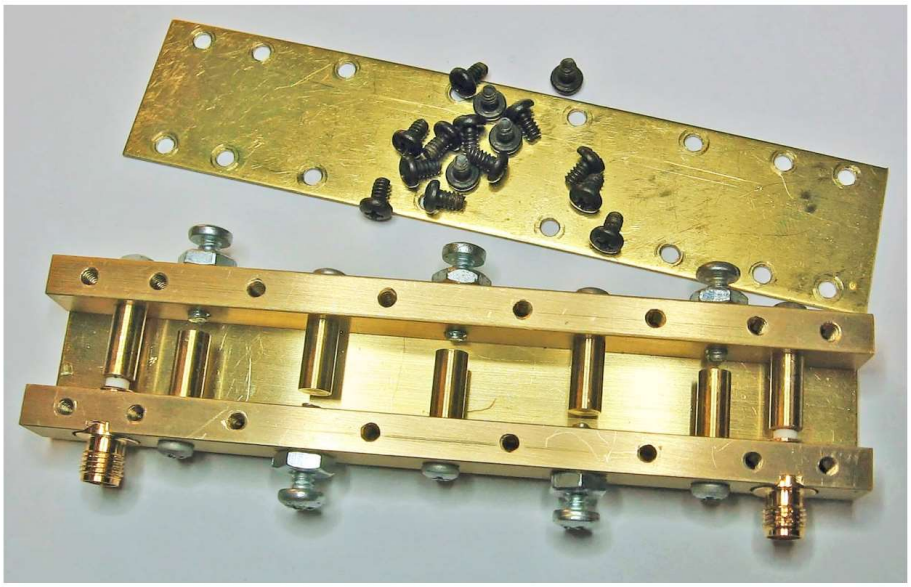

Figure 1 — INTRFIL 5 resonator interdigitated filter.

Introduction

INTRFIL began as an exercise to extend the interdigitated filter program that appeared in *Ham Radio* magazine in 1985 **[2]**. That program appears to correctly calculate the rod spacing but the input/output tap points appear to be more problematic, and its algorithms were not well documented. While this program produces very usable filters, I had to adjust the end rod taps in order to get the passband and ripple correct. In addition, tapping the input/output lines becomes more difficult as the frequency increases. Attempts to make filters in the 6 GHz region were a disappointment.

There is no real upper/lower frequency limit for filters made with *INTRFIL*, and 500 – 6000 MHz seems to be a reasonable range. The lower frequency is limited by how large you are willing to make the filter, and the upper frequency limit is set by how small you can make the resonators. *INTRFIL* uses input/output coupling rods rather than tapped resonators for the input/output. This requires two extra rods beyond the number of resonators but it allows for more controlled input/output coupling particularly at higher frequencies. *INTRFIL* is intended to create a filter design that has a high probability of success if you follow its results carefully. The simulation and test filters in this paper are intended to verify the design.

The filters created by *INTRFIL* are more complex than those using pipe caps or hair pin PCBs. While relatively easy to construct and tune, these filters offer modest performance in the stop band. For several microwave bands this is probably adequate as the mixing and LO spurious products from most transverters tend to fall in band. However, consider 2304 MHz. The LO and mixing products fall out of band for low side LO injection. These out of band emissions fall in the spectrum below 2300 MHz that is used by weak signal space and satellite systems. The

example 2304 MHz filter is capable of suppressing the out of band 2248 MHz mixing product for a 28 MHz IF by over 60 dB.

INTRFIL is written in Pascal programming language. The Free Pascal Compiler (FPC) **[3]** is a modern cross platform compiler. You can compile *INTRFIL* for Windows, MAC or Linux. In addition, there is a light weight, easy to use integrated development environment (IDE) called Geany **[4]** that makes running and/or editing *INTRFIL* source easy. *INTRFIL's* I/O is text in a terminal window with only minimal error checking. This is crude, but it works. My hope is someone with more advanced programming skills might write a nice GUI for *INTRFIL*.

The source code for *INTRFIL* is available **[5]** under General Public License (GPL). 32-bit Windows and Linux executables are available. While the GPL does not preclude commercial use, it means that *INTRFIL* is provided with no warranty. You use it at your own risk, and it can't

Screen dialog for INTRFIL *Required input information is printed in bold.*

INTRFIL: Interdigitated Filter Program Version 1.0
Copyright (c) 2021 Dennis G. Sweeney WA4LPR
Number of elements? 5
Center frequency (MHz) 5760
Butterworth (1) Chebychev (2) ? 2
Ripple Bandwidth (MHz) 30
Bandpass ripple (DB) 0.05
3 dB Bandwidth (MHz) = 35.26
Ripple Return Loss = 19.4 dB
Load impedance 50
ground plane spacing in = 0.375
rod dia in = 0.1875
d/h = 0.500 Slab Zo = 55.76
Coax Zo = 56.08
Calculated odd/even impedances and coupling coefficients

Zoo[0] = 46.81 Zoe[0] = 53.19
K = 0.0639
Zoo[1] = 49.62 Zoe[1] = 49.97
K = 0.0035
Zoo[2] = 49.67 Zoe[2] = 49.92
K = 0.0026
Zoo[3] = 49.67 Zoe[3] = 49.92
K = 0.0026
Zoo[4] = 49.62 Zoe[4] = 49.97
K = 0.0035
Zoo[5] = 46.81 Zoe[5] = 53.19
K = 0.0639

Odd/even impedances for fixed d/h = 0.500 with
s/h rod spacings

Zoo = 51.92 Zoe = 59.01
s/h[01] = 0.5953 c - c = 0.411 in
Zoo = 55.45 Zoe = 55.84
s/h[12] = 1.4481 c - c = 0.731 in
Zoo = 55.51 Zoe = 55.80
s/h[23] = 1.5238 c - c = 0.759 in
Zoo = 55.51 Zoe = 55.80
s/h[34] = 1.5238 c - c = 0.759 in
Zoo = 55.45 Zoe = 55.84
s/h[45] = 1.4481 c - c = 0.731 in
Zoo = 51.92 Zoe = 59.01
s/h[56] = 0.5953 c - c = 0.411 in

Parameters for filter cavity length = wavelength/4

Ct = 0.2016 pF; Cf = 0.1251 pF; Cp = 0.0765 pF
l = 0.386 in; gap = 0.081 in; lamda/4 = 0.512 in

Cavity spacing width can be adjusted ±10% of wavelength/4
Spacing = (in) 0.5

Parameters for Filter cavity

Ct = 0.1845 pF; Cf = 0.1251 pF; Cp = 0.0593 pF
New Ct Rod Length = 0.395 in
New gap = 0.105 in
Rod + gap = 0.500 in

Estimated resonator Q = 1040.2; Filter Q = 192.0
Loss = 5.27 dB

Data for simulation model using coupled lines

Zs = 111.52

Zooprime = 80.66 Zoeprime = 101.71
Zooprime = 89.40 Zoeprime = 90.54
Zooprime = 89.55 Zoeprime = 90.39
Zooprime = 89.55 Zoeprime = 90.39
Zooprime = 89.40 Zoeprime = 90.54
Zooprime = 80.66 Zoeprime = 101.71

Ct = 0.1845 pF; Bar length = 10.044 mm

Figure 2

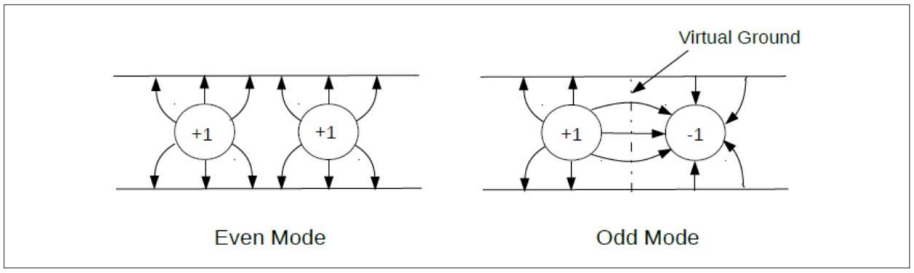

Figure 3 — Even and Odd Modes. With the even mode, each line is charged to the same potential and they have a characteristic impedance Zoe and for the odd mode they are charged to opposite potentials and the impedance is Zoo.

appear as some proprietary software. My intent is for anyone to be able to use it, and it is not intended as a commercial product.

Running *INTRFIL*

Figure 2 is the INTRFIL screen dialog for the 5760 MHz test filter. The required input parameters are shown in bold (bold is absent in the actual computer I/O). This example is for a 5-element 30 MHz wide (35 MHz is the bandwidth at the 3-dB points) 0.05-dB ripple Chebychev filter for 5760 MHz. It is intended for a 5760 MHz transverter with a 28 MHz IF. While designed for 5760 MHz, it was actually tuned for 5770 MHz as will be explained later. A 2304 MHz filter will be presented as well.

In order to run *INTRFIL*, you need to provide the parameters for the desired filter. You specify the number of resonators (elements) and the center frequency of the filter. The end bars are not resonators but provide the input/output coupling so a 5 resonator filter will have 7 bars. You then specify a Butterworth or Chebychev response. For a Chebychev filter, you will be asked for the bandwidth between equal ripple points and the band-pass ripple. The bandwidth for Chebychev filters is defined between equal ripple points and it is less than the 3-dB bandwidth. *INTRFIL* then calculates and reports the 3-dB bandwidth and the minimum in band return loss. If you specify a Butterworth filter, the bandwidth is the 3-dB bandwidth and no additional information is needed.

INTRFIL proceeds by requesting the load impedance. This is generally 50 Ω. *INTRFIL* then asks for the ground plane spacing and the rod diameter dimensions.

INTRFIL calculates and reports the diameter to ground plane spacing ratio, d/h, the impedance of the specified slab line and the impedance of an equivalent coax line. These data will be used later for the approximations that determine the rod capacitive loading and the resonator Q.

INTRFIL calculates rod coupling in terms of even and odd mode impedances depicted in **Figure 3**. The even/odd mode impedances for each set of coupled lines and the resulting coupling coefficient are calculated and printed. You could build a filter directly from these values, but each set of lines will have a different rod diameter.

INTRFIL then calculates a new set of even and odd mode impedances where the rod diameter is fixed, i.e., d/h is fixed. The algorithm uses the fixed d/h and the coupling coefficients calculated in the previous step to calculate the rod spacing, s/h. This is a compromise but it appears to work well for narrow-band filters where the coupling between adjacent sets of rods is fairly weak. From s/h and the rod diameter, *INTRFIL* calculates the center-to-center (c-c) distance for each set of rods.

Using the ¼ wavelength at the center frequency as the cavity wall spacing, *INTRFIL* estimates the rod length. The actual rod length is somewhat less than a ¼ wavelength. The rod is foreshorten by the fringing capacitance, Cf, formed by the open circuit at the end of the rod and by the parallel plate capacitance, Cp, formed by the gap between the end of the rod and the cavity wall. The total capacitive loading is the sum of these two capacitors. See **Figure 4**.

The ¼ wave dimension for the cavity may not be very convenient so you have the option of specifying a new cavity wall spacing. However, you are limited to a change of ±10% from the ¼ wave dimension. In the example above, the actual ¼ wavelength is 0.512 inches. A more convenient dimension would be 0.500 inches. That paired with ¼ inch thick side bars will result in 1.0 inch wide top and bottom covers. Covers for the test filter were made with a 0.032" by 1.0" brass strip obtained from K&S Precision Metals. K&S material is available in many hobby shops. With this new value of cavity spacing, *INTRFIL* goes back and recalculates the gap, a new capacitive loading (Cp), and the resulting rod length. This is shown in **Figure 4**.

An estimate of the resonator Q and filter loss is next reported. Measurement suggests that this estimate is optimistic but not unrealistic. Later in the paper is a discussion of the limitations of the loss estimate. *INTRFIL* also calculates a "filter Q." This is the ratio of center frequency to specified bandwidth. A rule of thumb is that resonator Q should be 10 times the filter Q for reasonable loss performance. This is not a requirement but it provides insight into loss performance.

Finally *INTRFIL* creates data for a simulation model using coupled lines. These data can be used in simulators like *QUCS* to create a simulation. Any simulator that has a single coupled line model should be able to employ these data to create an array of coupled lines that mimics the interdigitated structure. Information for creating this simulation is provided later in the paper.

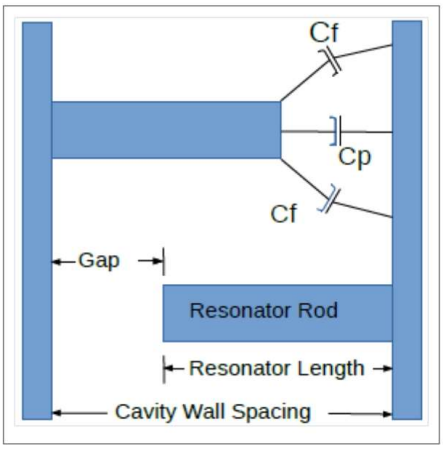

Figure 4 — Fringing capacitance, Cf, and parallel plate capacitance, Cp, are formed by the end of the resonator rod. INRFIL adjusts the gap and resonator length for small changes in the cavity wall spacing so as to maintain the chosen center frequency.

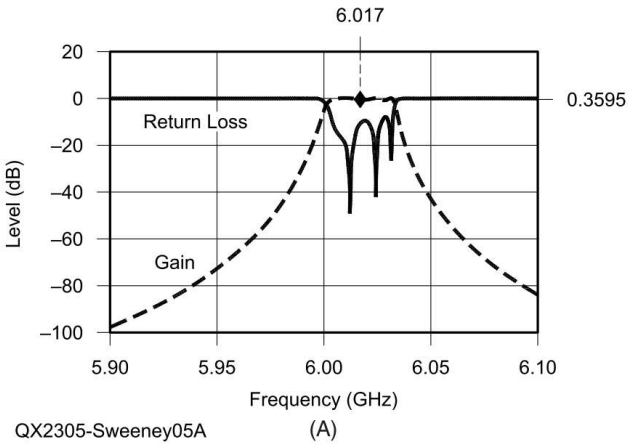

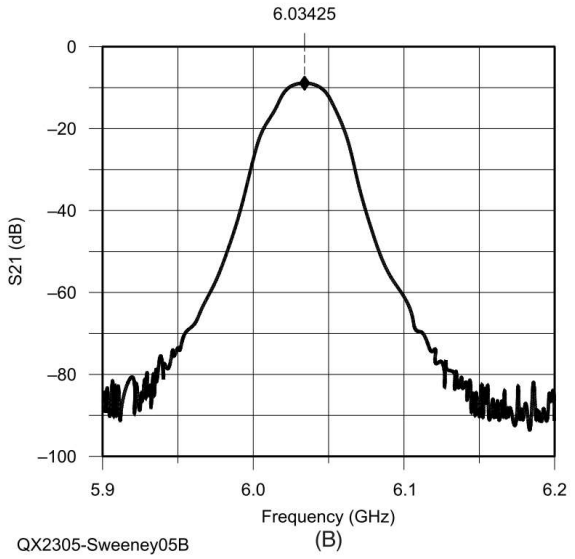

Figure 5 — The simulator plot (A) for 0.395" rods with 0.1845 pF capacitive loading. The simulator plot does not account for loss. (B) is the measured filter built to the same parameters. The simulated and measured center frequency is approximately 4.5% higher in frequency than requested. In the final test filter, the rods were lengthened 2.5% to 0.406" to make for easier tuning.

Center Frequency Approximation

The rods in interdigital filters are nominally a ¼ wavelength long at the filter center frequency. However in practice, the rods must be slightly shortened because they are loaded by the fringing capacitance at the open end of the rod and the parallel plate capacitor formed by the end of the rod and the side wall of the filter. The *INTRFIL* algorithm used to correct the rod length is an approximation. There does not appear to be a model for the fringing capacitance for slab line. However the work of Nicholson **[6]** uses a mathematical concept called conformal mapping **[7]** to convert the slab line into an equivalent coax line and then estimates the fringing capacity of that coax line. A 5th order polynomial curve fit is used to approximate Nicholson's fringing capacitance. The data were obtained by measuring the capacitance plot in Nicholson's paper with digital calipers and then doing a polynomial curve fit. The curve fit coefficients were obtained with *Octave's* polyfit. This works surprisingly well as it almost exactly reproduces Nicholson's example.

There is good agreement between the center frequency reported by the simulator and the measured center frequency of a built filter but these results suggest that Nicholson's algorithm makes a filter that comes out high in frequency. This is fortuitous as the filter can be tuned down with screws at the open end of the rods. The 2304 MHz filter, described later, came out high in frequency as well.

As already noted, *INTRFIL* gives you the option to slightly adjust the cavity width. You are limited to a change of ±10% from the ¼ wave dimension. With this new value of cavity spacing, *INTRFIL* goes back and recalculates the capacitive loading, a new rod length and the resulting gap between the rod end and the filter wall. To accomplish this, *INTRFIL* uses an iterative algorithm **[8]**. It will return a "failed to converge after 40 iterations" error message if it is not successful. You should not see this error as this

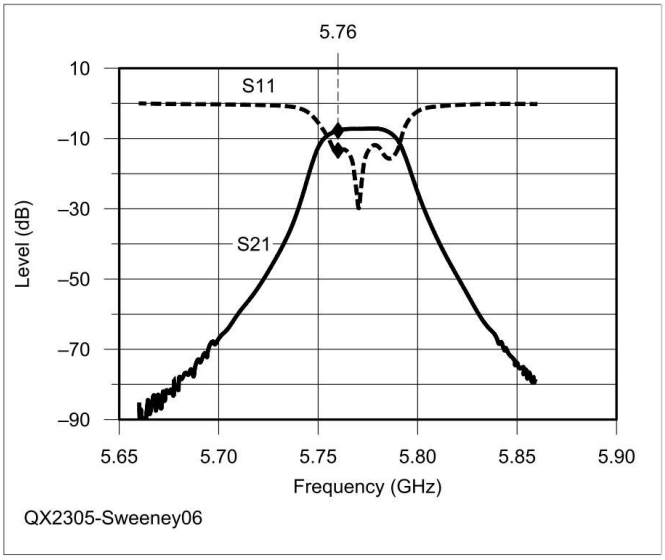

Figure 6 — Measured results for the completed filter. The measured 3-dB bandwidth is 36.96 MHz and the mid-band insertion loss is 7.5 dB. This filter was tuned to 5770 MHz so 5760 MHz is at the bottom of the passband. This filter is 33.4 dB down at 28 MHz removed from 5760 MHz and 56.5 dB down at 56 MHz removed.

algorithm, while slower than the algorithm described later for s/h, is mathematically guaranteed to converge to an answer. If this error appears, it likely that the estimate falls outside the range that the algorithm can test. This suggests that you attempted too large a change in cavity width. The reason for the ±10% limit is to limit the range over which the algorithm will work. There is some error checking to enforce this ±10% limit so you should never see this error.

The test filter center frequency was tuned to 5770 MHz with

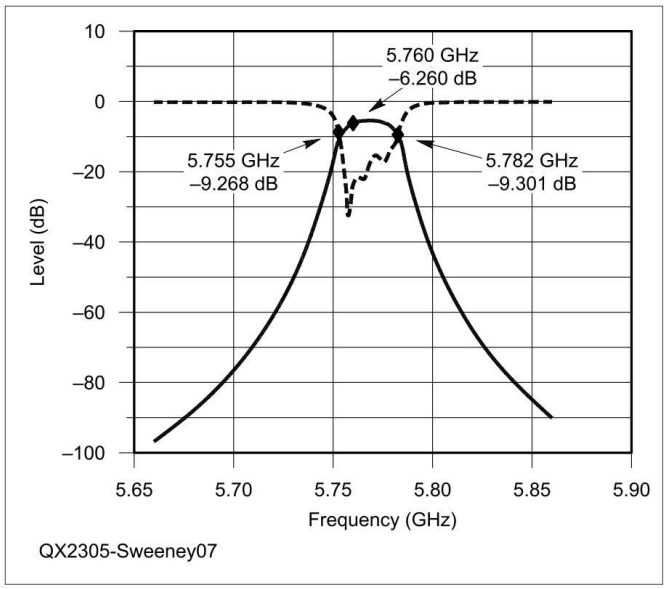

Figure 7 — Simulated results for the completed filter. Solid trace is gain, dashed trace is return loss.

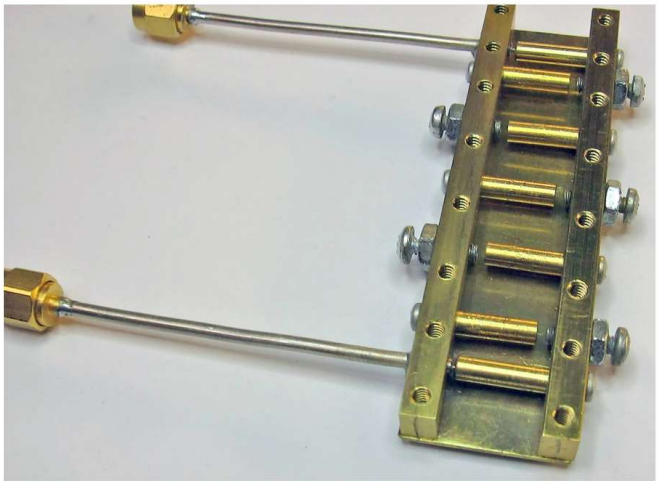

Figure 8 — 5.7 GHz filter fed with 0.085" semi-rigid cable soldered into the filter wall. This early filter was one with 0.125" rods secured with 2-56 screws.

the tuning screws. This is slightly high so 5760 MHz is at the lower end of the passband. This maximizes the LO and image rejection when using a 28 MHz IF.

The measured center frequency for the filter with the predicted 0.395" rods was 6034 MHz and the simulation reports 6017 MHz as the center frequency. See **Figure 5** for a *QUCS* simulation and the measured results of the filter built to the computer specification. The rods for this test filter were then lengthened 2.5% from the predicted 0.395" to 0.406" to make tuning easier. Cf does not change although with the longer rods Cp will be slightly larger. The simulator was used to check the center frequency. With the longer 0.406" rods, the measured untuned center frequency is approximately 5869 MHz and the simulator reported the center frequency as 5895 MHz.

Figure 5A simulator plot is for 0.395" rods with 0.1845 pF capacitive loading. The simulator plot does not account for loss. **Figure 5B** is the measured filter, with no tuning, built to the same parameters. The simulated and measured center frequency are approximately 4.5% higher in frequency than requested. It was possible to tune this filter down to 5770 MHz but, in the final test filter, the rods were lengthened 2.5% to 0.406" to make for easier tuning.

Needless to say at 5.7 GHz a few thousandths of an inch makes a difference but the simulator is useful in predicting the center frequency. The filter still needs to be tuned to get a flat passband. Filters this narrow will never be "no tune" although the filter with the 0.395" long rods has a surprisingly well formed passband with no tuning. Inevitably filters such as this must be tuned but their predicted center frequency should be close enough to allow for predictable tuning. It is even better if they have a reasonably formed passband without tuning. That way they can be tuned with a simple signal source. **Figures 6** and **7** are the measured and simulated results respectively for the completed filter tuned to 5770 MHz. **Figure 10** is a complete mechanical drawing for the 5760 MHz filter.

Figure 6 shows the measured results for the completed filter. The lower trace is the filter insertion loss (10 dB/division) and the upper trace is the return loss (5 dB/division). The measured 3-dB bandwidth is 36.96 MHz and the mid-band insertion loss is 7.5 dB. This filter was tuned to 5770 MHz so 5760 MHz is at the bottom of the passband. This filter is 33.4 dB down at 28 MHz removed from 5760 MHz and 56.5 dB down at 56 MHz removed. A return loss of 10 dB corresponds to a SWR of approximately 1.9:1.

Figure 7 shows the simulated results for the completed filter. The loading capacitors were trimmed on the simulator to move the frequency down to agree with the measured filter. The 3-dB bandwidth is 27 MHz. Filter loss was adjusted to reflect the loss predicted by the computer synthesis. Loss narrows the bandwidth as it tends to affect the edge of the passband more than the center. Without the loss, the simulated 3-dB bandwidth is 31 MHz. The *QUCS* simulation model used to create this plot is shown later in **Figure 14**. The filter rods were lengthened to 0.406" from the 0.395"reported for the simulation data in **Figure 2**.

Chebychev Bandwidth Specification

The band pass for Chebychev filters is defined between equal ripple points and that is less than the 3-dB bandwidth. When a Chebychev filter is specified, *INTRFIL* calculates the 3-dB bandwidth and the minimum in band return loss for the specified ripple. For passive lossless networks, power is either transmitted through the network or reflected from it. Formally this is:

$$1-|S_{21}|^2 = |S_{11}|^2$$

which is the ratio of the reflected power to the incident power. It is often referred to as return loss and given in dB. Since the ripple you specify for a Chebyshev filter is actually an insertion loss and given the lossless assumption, there will be a corresponding reflection. If you are lucky enough to have access to a network analyzer, return loss is a very sensitive way to

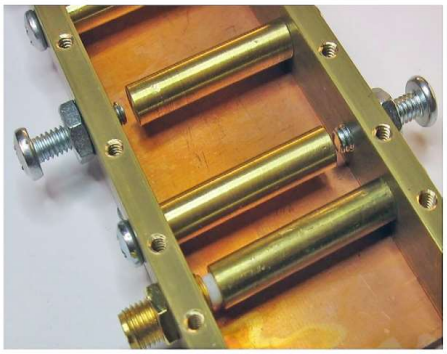

Figure 9 — 2.3 GHz filter fed with a SMA connector. The rods are 0.25" in diameter.

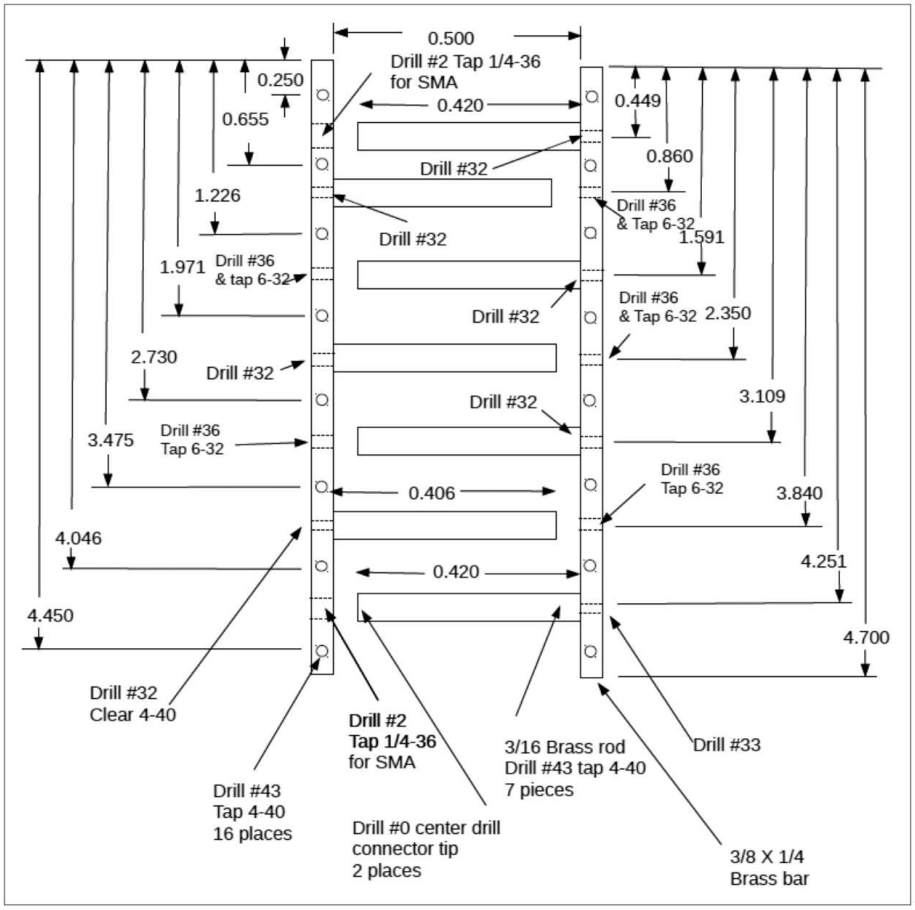

Figure 10 — Mechanical drawing for 5760 MHz test filter. While not specified in the drawing, the edge and side bar holes are located along the bar and side center line.

tune filters. Return loss is often specified as positive number of dB and, the larger the number, the better match. It is important to remember that it is actually a numerical ratio less than one and you need to know when to include the negative sign in dB calculations.

Resonator Q and Loss Approximation

INTRFIL estimates the resonator Q and calculates an approximate loss for the center of the passband. The Q approximation was developed by Nicholson **[9]** and it uses the equivalent coax line created by conformal mapping. Resonator Q is estimated on the basis of brass as the filter material but it is possible to edit *INTRFIL* to accommodate other materials. Brass is more lossy than silver but brass, copper and aluminum will probably be the most common construction materials. There is a note in the *INTRFIL* source code that tells you how to edit the code to accommodate a different construction material.

Resonator Q is used to estimate filter loss. 5.27 dB is the predicted loss for the 5.7 GHz test filter. The actual measured mid-band loss is approximately 7.5 dB. It is not surprising that the accuracy of this prediction degrades as the frequency increases. The loss estimate is more accurate for the 2.3 GHz filter described later.

Construction Thoughts

The easiest and most accurate way to create a filter is to use a lathe and a milling machine. The CNC machines, available in some Makerspaces, would be ideal but not all amateurs have access to such equipment. I have a manual table-top milling machine and a 60+ year old Atlas lathe (sold under the Sears, Roebuck name!). The lathe has a set of 3AT collets, which allow for precisely drilling and tapping the end of the small diameter rods used for the resonator rods.

It may be possible to get around the lack of machine shop facilities. I published a paper on making waveguide band-pass filters in *Microwave Update* 1989 **[10]**. A technique was outlined in that paper for precisely placing the posts in the waveguide using only a drill press and a set of calipers. I haven't tried it, but that technique might be adapted for making *INTRFIL* filters. A good set of calipers is a must. The rod length can be increased by the wall thickness and the filter wall drilled for the rod diameter. The rods can then be soldered in the side wall negating the need to drill and tap the end of the rod. However, getting the rod length accurate this way is more difficult. Find a friend with a lathe!

Most of the test filters were made with brass rods and copper/brass side walls. Standard sized material was used where possible. d/h = 0.5 is a convenient dimension and it creates slab lines close to 50 Ω. Material can be obtained on line. Most of my material came from Online Metals **[11]** but there are other vendors. The top and bottom plates in most of the test filters were made with brass K&S metal strips, printed circuit board (PCB) material or 0.05" aluminum sheet. PCB material results in a copper wall. The PCB top and bottom plates were trimmed to size with the milling machine. A word of caution when working with PCB material: the glass epoxy is very abrasive and it will quickly dull a file or a high speed steel mill cutter. I use a solid carbide mill cutter. It's more expensive but up to task.

Depending on rod size, the end of the rods are drilled and tapped for 2-56, 4-40 or 6-32 screws. 4-40, 6-32 and 8-32 screws were used for tuning screws. The top and bottom plates are held on with 4-40 screws. A lid screw is placed half way

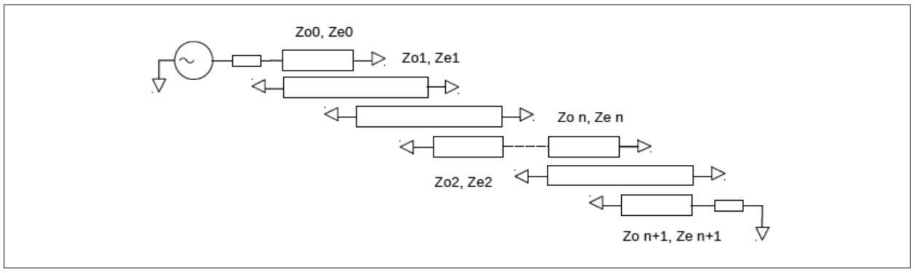

Figure 11 — Half-wave edge coupled filter with grounded ends.

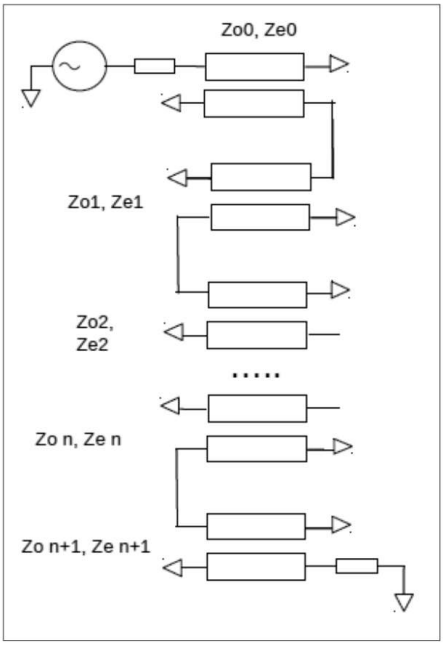

Figure 12 — Folder filter. Elements 0 and n+1 are the input/output coupling bars.

between each rod. Some early 5.7 GHz test filters used smaller 2-56 screws. Avoid these if possible as 2-56 taps are more expensive and break easily! There are a lot of holes and, if you break that small tap, it usually means you have to start over.

The ends of the filter are left open. If the side walls and top/bottom plate extend for a couple of rod diameters beyond the last rod, closing the end should have little effect. This doesn't seem to be critical.

Input/output can be done through either 0.085" or 0.141" semi-rigid coax soldered into the side wall, see **Figure 8**, or SMA connectors. If the side wall is more than 0.375" wide, you can drill and tap for an SMA connector. The connector should be threaded continuously over its entire length so it can be screwed into the side wall, see **Figure 9**. SMA connectors have a ¼-36 thread. While this thread is somewhat uncommon, taps are available. They can be found on eBay or at machinist supply houses like Victor Machinery Exchange **[12]**.

Be sure the connector is long enough to go through the side wall plus accommodate a lock nut and the SMA plug. It appears that SMA connectors threaded over their entire length are getting harder to find. A header rear mount connector from Jameco **[13]** part number 153286 was used for the 5760 MHz test filter. The side bar is 0.25" thick so the ¼-36 mounting hole had to be counter sunk about 0.06" to allow the end of the connector to came through. A close examination of **Figure 1** shows the counter sink.

Connectors similar to the Jameco part can be found on eBay. However, be careful of eBay connectors. Their insulation might not be PTFE. As a result they may be very lossy at microwave frequencies or they may have unexpected discontinuities.

One end of an end coupling rod will be drilled and tapped for a screw to hold it to the side wall. The other end is drilled with a small center drill (#0) so the center pin of the SMA connector or the center conductor of the coax can be soldered into the hole. That way the connector or the coax can be connected to the coupling rod with a minimum of discontinuity. Since the coupling rod is a not a resonator, its length is less critical. Adjusting its length is one way to optimize the connector projection. A close examination of the mechanical drawing in **Figure 10** shows that coupling rods were lengthened from 0.406" to 0.420".

Internal to *INTRFIL*, all dimensions are calculated in cm but the dimensions are reported in inches. (My apologies to my metric colleagues.) You can obtain metric dimensions by editing everywhere *INTRFIL* has 2.54 and replacing it with 1.0 and replacing all the "in" labels with "cm". *INTRFIL* reports the rod length in mm in the simulation data because the *QUCS* coupled line model specifies the line length in mm.

Figure 10 is the mechanical drawing for the 5760 MHz test filter. It is dimensioned in such a way that it uses the bar end as the reference and the dimensions are accommodated by advancing the mill table. The mill has a digital readout that makes this accurate and relatively easy.

Inside *INTRFIL*

INTRFIL is built around the algorithm published by Matthaei **[14]** for an edge coupled filter as shown in **Figure 11**. The resonators are ½ wavelength long and their ends are grounded. The Matthaei paper also has an algorithm for the dual of this filter where the ends of the resonators are open circuited. That topology is probably more common in amateur use.

An examination of this structure suggested that it might be modified to make an interdigitated filter by folding it in half as shown in **Figure 12**.

While not immediately obvious, this doubles the bandwidth because the filter impedance is cut in half. The ¼ wave sections that were once in series are now in parallel. This was discovered almost by accident while simulating the interdigitated implementation of this filter. To correct for this, *INTRFIL* simply divides the bandwidth you specify by two.

The dimensions for an interdigitated filter are usually determined by the capacity to ground and the rod to rod capacity of each set of rods. The classic way to do this is from the graphs of E. G. Cristal **[15].** Unfortunately this creates different sized rods for each set of resonators and the graphs do not lend themselves to computer aided design. Vadopalas and Cristal **[16]** suggest that approximations for even and odd mode impedances could be used to analytically synthesize the rod to ground and rod to rod capacitance. This could be the basis for a computer algorithm. *INTRFIL* does not require this step. The folded version of *INTRFIL* is already defined by its even and odd mode impedances.

Using the even and odd mode impedances, *INTRFIL* calculates the coupling coefficient, *K*, between pairs of rods:

$$K = \frac{Zoo - Zoe}{Zoo + Zoe}$$

It is possible to enforce equal diameter

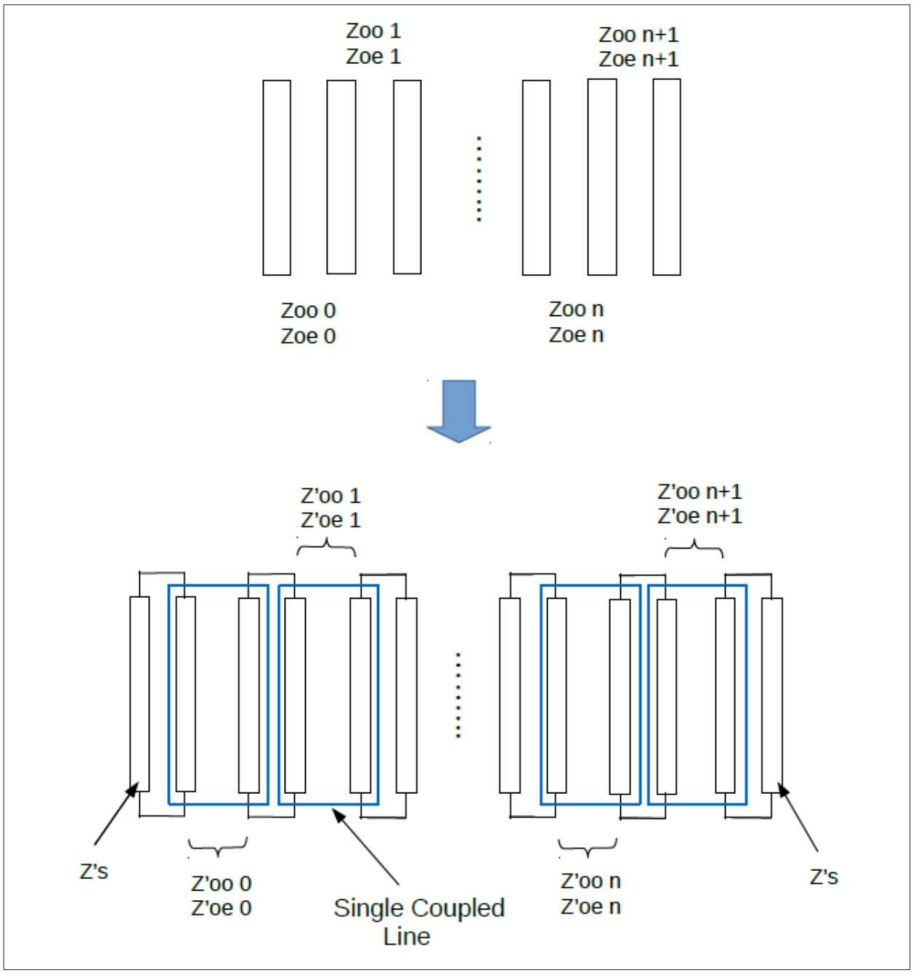

Figure 13 — Synthesis of coupled line model for simulating an interdigitated filter.

rods and adjust rod spacing, s/h, to obtain new even and odd mode impedances that produce the same value of *K*. However, this compromises the internal impedance of the filter. Simulation suggests that this has little effect for narrowband filters where the coupling between rods is relatively weak and where the difference between the two different sets of impedances is not that great. Exactly where this approximation breaks down is not known. Filters for amateur use tend to be fairly narrowband. Some 5-element 5% BW filters made for 1900 MHz exhibited an unexpected decrease in return loss (poorer match) in the center of the passband. The narrowband test filters in this paper did not show this decrease in return loss. This suggests that the internal coupling in the wider band filters may not be correct. The bandwidth and response of these wider band filters were very close to the prediction and they were still quite usable filters. Similar wide-band 3-element filters did not exhibit this effect. It is not clear if this is related to the filter synthesis, to the tuning, or to construction anomalies. This might be an exercise for the simulator.

A computer algorithm that calculates the even and odd mode impedance of a pair of coupled lines from d/h and s/h is implemented in *INTRFIL* **[17]**. This algo-

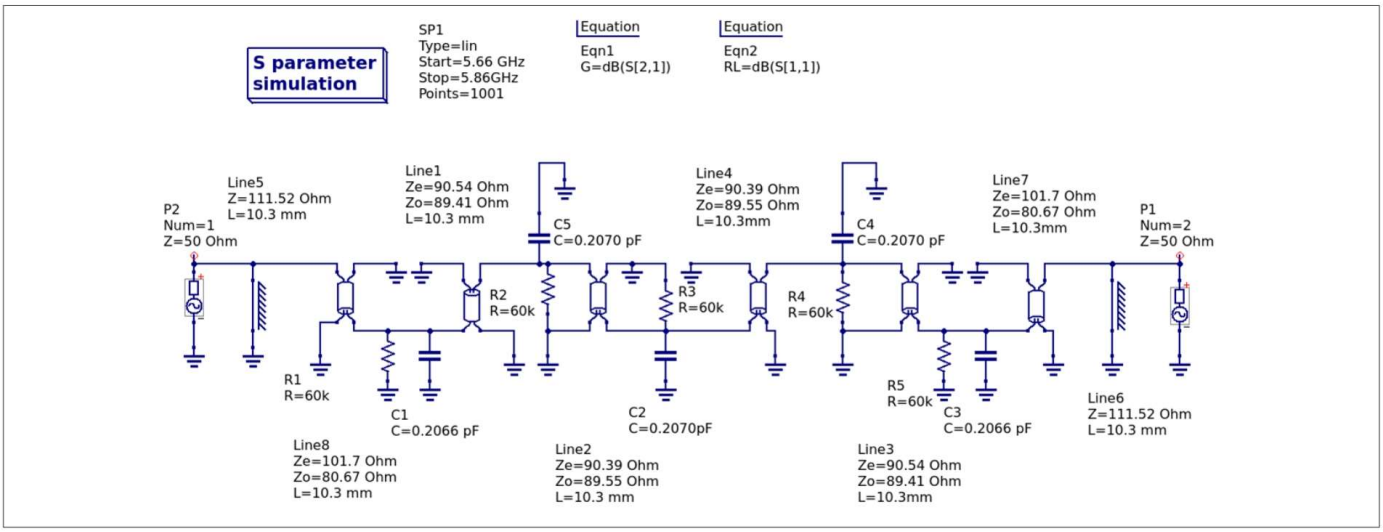

Figure 14 — QUCS simulation for the 5-element 5760 MHz filter example using an array of parallel coupled lines.

rithm calculates *Zoo/Zoe* from rod dimensions.

Here is where *INTRFIL* has to do some heavy computing. You have *K* and d/h but not the rod spacing, s/h. *K* is a function of *Zoo/Zoe*, which are a complex function of d/h and s/h:

$$K = f(Zoo, Zoe) = f(\text{d/h}, \text{s/h})$$

Given the complexity of the *Zoo/Zoe* algorithm there is no direct way to solve for s/h. *INTRFIL* uses an iterative numerical technique **[18]** that creates values for s/h until the difference between the computed value of the coupling coefficient *K* and the original value of *K* is less than a specified error. For some values of d/h, s/h or *K*, this algorithm may not converge properly to an answer. The resulting s/h and *Zoo/Zoe* may still be usable but with reduced precision. The simulator can

Screen dialog for INTRFIL *Required input information is printed in bold.*

INTRFIL: Interdigitated Filter Program Version 1.0
Copyright (c) 2021 Dennis G. Sweeney WA4LPR

Number of elements? 5
Center frequency (MHz) 2310
Butterworth (1) Chebychev (2) ? 2
Ripple Bandwidth (MHz) 30
Bandpass ripple (DB) 0.05
3 dB Bandwidth (MHz) = 35.26
Ripple Return Loss = 19.4 dB
Load impedance 50
ground plane spacing in = 0.5
rod dia in = 0.25

d/h = 0.500 Slab Zo = 55.76
Coax Zo = 56.08

Calculated odd/even impedances and coupling coefficients

Zoo[0] = 44.97 Zoe[0] = 55.03
K = 0.10056
Zoo[1] = 49.07 Zoe[1] = 49.93
K = 0.00871
Zoo[2] = 49.18 Zoe[2] = 49.81
K = 0.00643
Zoo[3] = 49.18 Zoe[3] = 49.81
K = 0.00643
Zoo[4] = 49.07 Zoe[4] = 49.93
K = 0.00871
Zoo[5] = 44.97 Zoe[5] = 55.03
K = 0.10056

Odd/even impedances for fixed d/h = 0.500 with s/h rod spacings

Zoo = 49.67 Zoe = 60.78
s/h[01] = 0.4607 c - c = 0.480 in
Zoo = 55.14 Zoe = 56.11
s/h[12] = 1.2009 c - c = 0.850 in
Zoo = 55.28 Zoe = 55.99
s/h[23] = 1.2854 c - c = 0.893 in
Zoo = 55.28 Zoe = 55.99
s/h[34] = 1.2854 c - c = 0.893 in
Zoo = 55.14 Zoe = 56.11
s/h[45] = 1.2009 c - c = 0.850 in
Zoo = 49.67 Zoe = 60.78
s/h[56] = 0.4607 c - c = 0.480 in

Parameters for filter cavity length = wavelength/4

Ct = 0.2674 pF; Cf = 0.1668 pF; Cp = 0.1005 pF
l = 1.103 in; gap = 0.110 in; lamda/4 = 1.277 in

Cavity spacing width can be adjusted ±10% of wavelength/4
Spacing = (in) 1.25

Parameters for Filter cavity

Ct = 0.2485 pF; Cf = 0.1668 pF; Cp = 0.0817 pF
New Ct Rod Length = 1.115 in;
New gap = 0.135 in
Rod + gap = 1.250 in

Estimated resonator Q = 1058.1; Filter Q = 77.0
Loss = 2.08 dB

Data for simulation model using coupled lines

Zs = 111.52

Zooprime = 75.36 Zoeprime = 108.63
Zooprime = 87.61 Zoeprime = 90.40
Zooprime = 87.97 Zoeprime = 90.03
Zooprime = 87.97 Zoeprime = 90.03
Zooprime = 87.61 Zoeprime = 90.40
Zooprime = 75.36 Zoeprime = 108.63

Ct = 0.2485 pF; Bar length = 28.322 mm

Figure 15

validate the results. *INTRFIL* returns a "failed to converge" error if the algorithm does not converge correctly. This error shouldn't occur very often but slight changes in bandwidth and/or ripple usually correct the problem.

Simulation

The ability to simulate a filter was an important part of the development of *INTRFIL* and it is useful for verifying the results generated by *INTRFIL*. It allows trimming the resonator length and/or the loading capacitors and checking filter bandwidth. Design followed by simulation followed by construction and measurement was the work flow. Good agreement between simulation and measurement gives one confidence in the design. Once there is confidence in the design, filters can be built without sophisticated test equipment.

Simulators such as *QUCS* have a model for a single pair of coupled lines. It is necessary to create an array of coupled lines that model the filter. This can be done with the technique outlined in **[19]**.

Single coupled lines are connected in parallel to create the array. The even and odd mode impedances are adjusted to accommodate this parallel connection. *INTRFIL* calculates these new impedances for the parallel connection as *Z'oo* and *Z'oe*:

$$Zs = slabZo$$

$$Z'oe = \frac{1}{\left(\frac{1}{Zoe} - \frac{1}{2Zs}\right)}$$

$$Z'oo = \frac{1}{\left(\frac{1}{Zoo} - \frac{1}{2Zs}\right)}$$

The model requires an extra transmission line at the input/output to balance the array. Its impedance is given by:

$$Z's = 2slabZo$$

where *slabZo* is the impedance of the slab

Table 1: 5760 MHz Test Filter.

	Design	Simulation	Measured
3-dB bandwidth	35.26 MHz	31.0 MHz w/o loss	36.96 MHz
Loss	5.27 dB	–	7.5 dB
Center frequency	5760 MHz	6017 MHz (6034 MHz measured)	Tuned to 5770 MHz
Rod Length	0.395"	0.395"	0.406"

Table 2: 2310 MHz Test Filter.

	Design	Simulation	Measured
3-dB bandwidth	35.26 MHz	31.3 MHz w/o loss	35.92 MHz
Loss	2.08 dB	–	2.17 dB
Center frequency	2310 MHz	2371 MHz (2359 MHz measured)	Tuned to 2310 MHz
Rod Length	1.115"	1.115"	1.124"

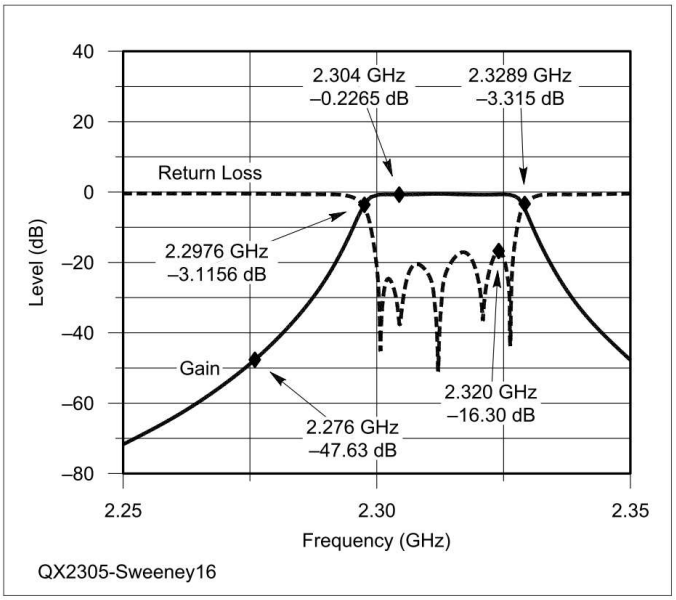

Figure 16 — Simulated response of the 2310 MHz test filter. The simulated 3-dB BW is 31.3 MHz. The rods were lengthened approximately 0.009" to 1.124" (approximately 1%) and the loading capacitors trimmed. No loss was added to this simulation.

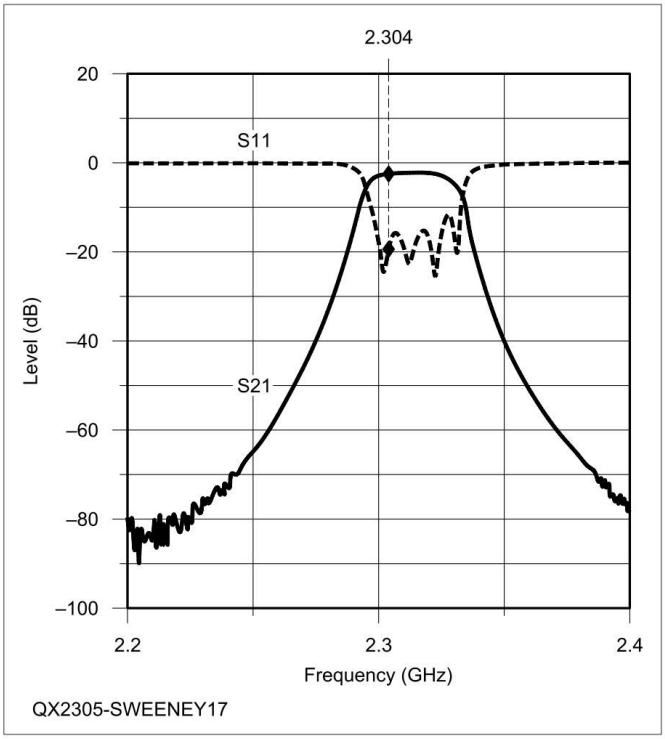

Figure 17 — Measured response of the 2310 MHz test filter. The measured 3-dB bandwidth is 35.92 MHz and the mid-band loss is 2.17 dB. The LO at 2276 MHz for a 28 MHz IF is attenuated 36.5 dB. The image frequency at 56 MHz below 2304 MHz is attenuated 63.5 dB.

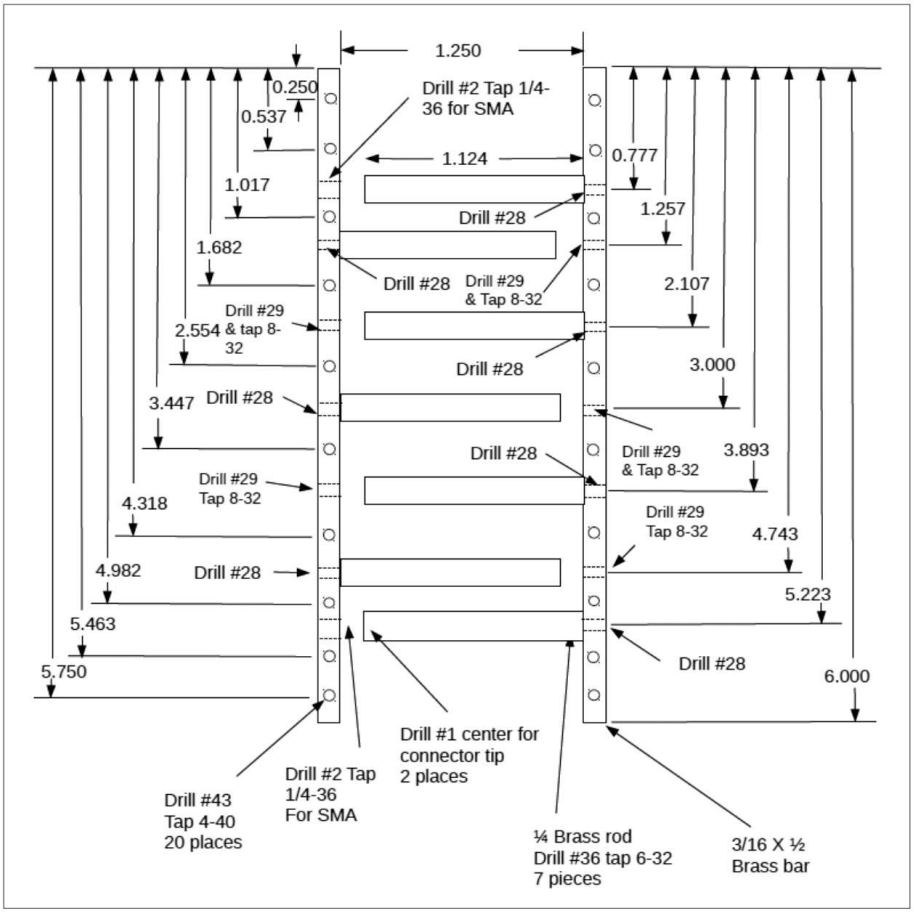

Figure 18 — Mechanical drawing for 2310 MHz test filter.

line reported by *INTRFIL* for the specified d/h.

The array is shown in **Figure 13**. As part of the synthesis process *INTRFIL* calculates all required values for the simulation. An implantation of a *QUCS* simulation is shown in **Figure 14**. The simulation is based on all the pairs of lines being the same impedance as the specified slab line. This can be checked by:

$$slabZo = \sqrt{(Zoo)(Zoe)}$$

The largest error occurs for the end pair of rods since they are the tightest coupled. However, the error is only a few tenths of an ohm.

Figure 14 shows the *QUCS* simulation for the 5 element 5760 MHz filter example using an array of parallel coupled lines.

The line impedances for this simulation were obtained from the "Data for simulation model using coupled lines" in **Figure 2**. C1 – C5 are the rod end capacitances and they were manually adjusted to tune the filter. You can use the value Ct reported by the computer as starting point. R1 – R5 simulate loss although there is a line loss parameter in the *QUCS* coupled line model that could be used instead. The resistor values were adjusted empirically to simulate the loss calculated by *INTRFIL*.

2304 MHz Filter

A second test filter was constructed using *INTRFIL*. The screen dialog is seen in **Figure 15** for convenience, and is the *INTRFIL* input/output for this filter. It is a five element 30 MHz wide (at equal ripple points) 0.05-dB ripple Chebychev filter for 2310 MHz. It is intended for a 2304 MHz transverter with a 28 MHz IF. It is tuned to 2310 MHz so 2304 MHz is at the low end of the passband. This maximizes the attenuation of the LO and image frequencies. The simulated and measured response of this filter are **Figures 16** and **17** respectively.

The cavity width was adjusted to 1.25" from the ¼ wave dimension of 1.277".

Figure 16 shows the simulated response of the 2310 MHz test filter. The simulated 3-dB BW is 31.3 MHz. The rods were lengthened approximately 0.009" to 1.124" and the loading capacitors trimmed. This increase in rod length is approximately 1%. No loss was added to this simulation. With the 1.115" rods originally predicted by the computer (and no tuning), the simulated center frequency was approximately 2371.0 MHz and the actual measured center frequency of the test filter without tuning was 2359 MHz. This is ~2.0% high. Even with 1.115" rods this filter tuned down to 2310 MHz easily.

Figure 17 is the measured response of the 2310 MHz test filter. The upper (at the center) trace is the filter response and the lower (at the center) trace is the return loss. The measured 3-dB bandwidth is 35.92 MHz and the mid-band loss is 2.17 dB. The LO at 2276 MHz for a 28 MHz IF is attenuated 36.5 dB. The image frequency at 56 MHz below 2304 MHz is attenuated 63.5 dB.

Figure 18 is a mechanical drawing for 2310 MHz test filter. While not specified in the drawing, the edge and side bar holes are located along the bar and side center line.

Conclusion

INTRFIL creates interdigitated bandpass filters using ¼ wavelength long round rods between parallel ground planes. **Table 1** and **Table 2** summarize the designed, simulated results, and measured results for the two test filters, one for 5760 MHz and the other for 2310 MHz.

The 5760 MHz filter had significantly higher loss than predicted but the agreement between design, simulation and measurement is encouraging. The 5760 MHz filter has a passband at 6034 MHz with the shorter rods and no tuning. The 2310 MHz filter with the short 1.115" rods had an almost perfectly formed passband centered on 2359 MHz with no tuning. All the rods in the 2310 MHz filter were ±0.001" of the 1.115". Precision is important but the results were encouraging enough that you could build a filter from the computer design and have confidence in its performance without sophisticated test equipment.

This article shows how to use *INTRFIL* and obtain useful results. It provides some

insight into how *INTRFIL* operates. Finally, a simulation technique is presented. Network simulators like *QUCS* offer a way to build your filter in the computer and verify its performance.

INTRFIL should be useful in designing filters in the 500 to 6000 MHz range that will satisfy almost any amateur need.

Dennis Sweeney, WA4LPR, was first licensed as novice, WN4LPR, in the summer of 1963. He subsequently upgraded to Technician, Advanced, and now Amateur Extra class. He is currently retired faculty from VA Tech in Blacksburg, VA. His last job was managing the undergraduate lab program for VA Tech's Electrical and Computer Engineering Department. He taught electronics, satellite communications and radio engineering. He also worked with satellite systems for the Aerospace Corporation. Dennis holds a PhD in electrical engineering and is a Senior Member of the IEEE. He is active on 6 m, 70 cm, 23 cm, and 3 cm using home brew equipment. He enjoys building things. Dennis is one of the founding members of the Blue Ridge Microwave Society.

References

[1] *QUCS*: Quite Universal Circuit Simulator. There appear to be three flavors of *QUCS*, the original *QUCS* (**http://qucs.sourceforge.net/**), *Qucs-S*: *QUCS* with *SPICE* (**https://ra3xdh.github.io/**) and *QucsStudio* (**http://dd6um.darc.de/QucsStudio/**). All three are available for free download but their licensing and development trajectories are different. *QucsStudio* appears to be the most developed. It has a nonlinear simulator, an EM simulator and a neat "tuning" function with sliders. However, it does not appear to be open source and it is currently available only for Windows. The others have a Windows, MAC and Linux variant and are available under General Public License (GPL). *QUCS* has a fairly steep learning curve but there are on line tutorials. The simulations in this paper were all generated using the original *QUCS* as I am primarily a Linux user.

[2] Jerry Hinshaw, N6JH, and Shahkrokh Monemzadeh, computer-aided interdigital bandpass filter design, *Ham Radio*, Jan. 1985, pp. 12-26.

[3] **https://www.freepascal.org/**

[4] **www.geany.org/**

[5] The source code and compiled versions are available from the Blue Ridge Microwave Society (BRMS) group site **groups.io/g/brms**. Look under the "Files" tab and then "Microwave Filters." The WGFIL waveguide filter program mentioned below is also available there.

[6] B.F. Nicholson, "The Resonant Frequency of Interdigital Filter Elements," IEEE Transaction on Microwave Theory and Techniques, Vol. MTT-14, No. 5, May 1966, pp. 250-251.

[7] Huang Hui, Liu Xinmeng, and Lv Sin, "Optimal Design of Precision Slab-line for N Type Coaxial Automatic Tuner," 79th ARFTG Microwave Measurement Conference, Montreal, Canada, 22-22 June 2012.

[8] Flannery, Teukolsky, Vetterling, *Numerical Recipes in Pascal*, Cambridge University Press, Cambridge, 1989, p. 277.

[9] B. F. Nicholson, "Dissipation Loss in Interdigital and Combline Filters," *Electronics Letters*, March 1966, Vol. 2, No. 3, pp. 90-91.

[10] Dennis G. Sweeney, WA4LPR, "Design and Construction of Waveguide Bandpass Filters," Proceedings of the Microwave Update 1989, pp. 124-134. The WGFIL waveguide filter program and an edited version of the paper are available from the Blue Ridge Microwave Society group site **groups.io/g/brms** or on Paul Wade's website: **www.w1ghz.org/**.

[11] **https://www.onlinemetals.com/**

[12] **https://www.victornet.com/**

[13] **https://www.jameco.com/**

[14] George L. Matthaei, "Design of Wide-Band (and Narrow-Band) Band-Pass Microwave Filters on the Insertion Loss Basis," IRE Transaction on Microwave Theory and Techniques, Nov. 1960, pp. 580-593.

[15] Edward G. Cristal, "Coupled Circular Cylindrical Rods Between Parallel Ground Planes," IEEE Transaction on Microwave Theory and Techniques, July 1964, Vol. MTT-12, Issue 4, pp. 428-439.

[16] P. Vadopalas and E.G. Cristal, "Coupled Rods Between Ground Planes (Correspondence), " IEEE Transaction on Microwave Theory and Techniques, Mar. 1965, Vol. MTT-13, Issue 2, pp. 254-255.

[17] Rosloniec, Stanislaw, *Algorithms for Computer-Aided Design of Linear Microwave Circuits*, Artech House, 1990, pp. 203-208; also Stanislaw Rosloniec, "An Improved Algorithm for the Computer-Aided Design of Coupled Slab Lines," IEEE Transaction on Microwave Theory and Techniques, Vol. MTT-37, No. 1, Jan. 1989, pp. 258-261.

[18] Lee W. Johnson, and R. Dean Riess, *Numerical Analysis*, 2nd Ed, Addison-Wesley Publishing, Massachusetts, 1982, pp. 166-168; also Flannery, Teukolsky & Vetterling, *Numerical Recipes in Pascal*, Cambridge University Press, Cambridge, 1989, University Press, Cambridge, 1989, Section 9.2.

[19] Carl Denig, "Using Microwave CAD Programs to Analyze Microstrip Interdigital Filers," *Microwave Journal*, Mar. 1989, pp. 147-152.

Upcoming Conferences

Aurora '23 Conference

June 3, 2023

Plymouth, MN

www.nlrs.club

Aurora '23 will be held June 3, 2023, at the West Medicine Lake Community Club in Plymouth, Minnesota

2023 Central States VHF Society Conference

July 27 – 30, 2023

North Little Rock, AR

http://2023.csvhfs.org

Central States VHF Society 2023 Conference will be held July 23 – 30, 2023 at the Wyndham Riverfront Little Rock, North Little Rock, Arkansas

Russ Ward, W4NI
4224 Brush Hill Rd., Nashville, TN 37216 | **w4ni@arrl.net**

Digital Filter Design Using *Octave*

An example illustrates the filter design process.

Digital filter design has two parts. The first part, addressed here, is deriving a set of decimal fractions. The second part is using those decimal fractions in a processor circuit.

A digital filter comprises three parts. The first part is an analog to digital converter (ADC) with which one periodically measures the input signal and passes that value to the processor. The second part is calculation by the processor with a set of recent input samples. The third part is a digital to analog conversion (DAC) of the processor calculation result as filter output. Filtering action is accomplished by multiplying the set of signal samples by the set of decimal fractions and summing the results for output. Determination of this set of decimal fractions is the subject of this note.

Gathering the set of input signal samples is controlled by the ADC sampling rate, a crucial frequency in filter design. Harry Nyquist proved that the sampling rate must be greater than twice the highest filtered frequency. For example, if the highest filtered frequency is 3 kHz, then the ADC sample rate must be at least 6 kHz. The processor must perform the filter calculations at this same sampling rate.

A second important filter design parameter is the number of input samples to be used concurrently. This is not a critical number, but consider that more samples means more stop-band depth. Since the Arduino Uno processor has 32 registers in the Arithmetic Logic Unit (ALU), and your author prefers to write programs in assembly language, good results have been obtained by using 27 registers to hold 27 input samples.

The *Octave* language is free on the web and provides useful functions for filter design. It is easy to download and install, but make sure to also get the free Signal Processing library extension.

A digital filter can be crudely viewed as a signal tube with a series of equally spaced taps providing signal samples. Think of the degree of opening of each tap as a tap weight. These tap weights are the decimal fractions described above as providing the actual filtering action. Adding the product of each tap weight times the corresponding sample determines the filter output value.

One may use *Octave* in either a command line or program invocation mode The low-pass filter is a first example.

First, invoke the Signal library:
PKG LOAD SIGNAL

Next enter Sampling Frequency in hertz:
SF=10000Now find tap weights for a low-pass filter:
LPTW=FIR1(26,0.5)

The FIR in the FIR1 function refers to Finite Impulse Response, which is one of the two main types of digital filters. The 26 in the first parameter actually gives 27 tap weights. Note that the tap weight number must be an odd number. The 0.5 in the second parameter is 0.5 or half of the maximum filter design frequency, which is itself half of the sampling frequency. This low-pass filter will have a cutoff frequency of 0.5 × 0.5 × SF = 2500 Hz.

Octave will calculate the required low-pass tap weights into variable LPTW.

To find frequency response use:
[LPM,LPF]=FREQZ(LPTW)
where LPM is low-pass magnitude response and LPF is low-pass frequency response.

Put LPM in a useable decibel format:
LPMDB=20*LOG10(ABS(LPM))
then plot the filter response:
PLOT((SF/2)*(LPF/PI),LPMDB)

Add documentation:
TITLE("Lowpass Response","FONTSIZE",25)
XLABEL("Frequency Hz","FONTSIZE",18)
YLABEL("Magnitude dB","FONTSIZE",18)

One can use the command:
HELP FIR1 to find information and syntax for other filters, such as:

HPTW=FIR1(26,0.5, "HIGH") for a high-pass filter. Frequency response is found similarly as with low-pass filter above.

The FIR2 function allows more design complexity. One designates frequency ranges in pairs along with a magnitude at each band edge. How about a CW band-pass filter with a 450 Hz to 600 Hz pass band?

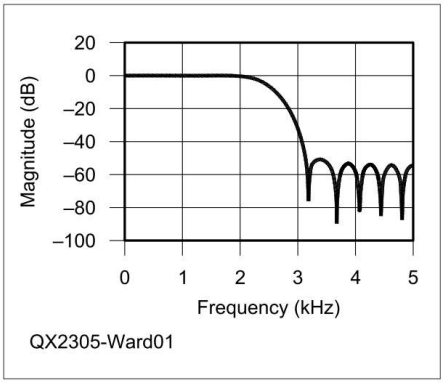

Figure 1 — Low-pass response.

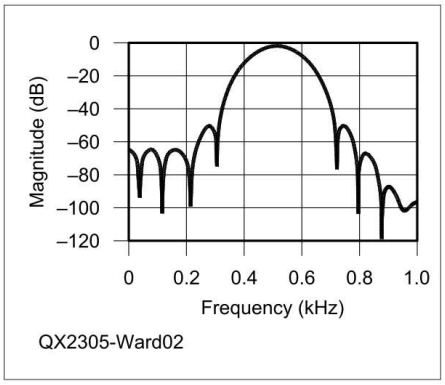

Figure 2 — Band-pass response.

```
    PKG LOAD SIGNAL
    SF=2000
    FR=[0,0.45,0.45,0.6,0.6,1]
    MAG=[0,0,1,0.9,0,0]
    BPTW=FIR2(26,FR,MAG)
    [BPM,BPF]=FREQZ(BPTW)
    BPMDB=20*LOG10(ABS(BPM))
    PLOT((SF/2)*(BPF/PI),BPMDB)
TITLE("Bandpass Response",
    "FONTSIZE",25)
XLABEL("Frequency Hz",
    "FONTSIZE",18)
YLABEL("Magnitude dB",
    "FONTSIZE",18)
```

Figure 1 shows the low-pass response, and **Figure 2** shows the band-pass response.

Please note the "customized" upper cutoff response (0.9) in the Magnitude definition and the plot. Normal value is 1.0. Deriving the filter tap weights is the first part of digital filter design. Now one uses those weights in a program on the processor of user's choice. Many types of microcontrollers include an ADC. One may safely disregard the smaller half of the nine decimal digits provided by *Octave* for the tap weights. The DAC function can be provided cheaply and simply by an R – 2R ladder circuit.

It is standard practice to include a comment on every line of a computer program, but education clarity has been provided by the interspersed text.

Russ Ward, W4NI, was first licensed in 1967 as WA4ZZU, then received the W4NI call sign in 1996. He has earned DXCC, WAC and WAS, and is Life member of ARRL. Russ has been volunteer examiner since 1986 with the Nashville VE team. He operates HF contests using phone and CW. His previous QEX *article was 30 years ago.*

Keith Stammers, GØSXG
12, Ballfield Lane, Kexborough, South Yorkshire, S75 5EF, England | **ks-radio@runbox.com**

A Graphical Method to Determine the Impedance of a Parallel Resistor and Reactance

A graphical solution to the parallel resistance and reactance problem.

In the September/October 2022 edition of *QEX* Eric Nichols' Self-Paced Essay #13 included an invitation for readers to explain the graphical solution of the parallel impedance problem shown in his Figure 4. I attempt to do that here for his inductive reactance example, although the result is the same for a capacitive one.

It is instructive to derive the mathematical expression for the parallel impedance, and from **Figure 1(A)** we find it to be:

$$Z = \frac{jX_pR_p}{R_p + jX_p} = \frac{jX_pR_p\left(1 - jX_p\right)}{R_p^2 + X_p^2}$$

or

$$Z = \left[\frac{R_pX_p}{R_p^2 + X_p^2}\right]\left(X_p + jR_p\right) \quad (1)$$

Note that I format **Eqn (1)** as a complex number modified by a scaling factor.

Obviously, the phase angle is

$$\tan\left(\theta\right) = \frac{R_p}{X_p}$$

which will be negative for a capacitive reactance, and

$$\left|Z\right| = \left[\frac{R_p.X_p}{R_p^2 + X_p^2}\right].\sqrt{\left(X_p^2 + R_p^2\right)}$$

or

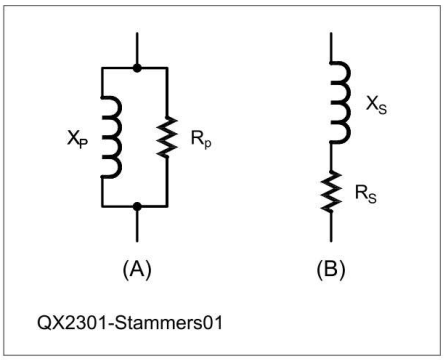

Figure 1 — (A) the parallel combination of reactance and resistance to be analyzed. Although an inductance is shown, the use of capacitance produces the same result, with just the phase angle becoming negative. (B) the equivalent series circuit that can be designed to have the same impedance and phase angle as the parallel combination.

$$\left|Z\right| = \frac{R_pX_p}{\sqrt{R_p^2 + X_p^2}}$$

The expression $(X_p + jR_p)$ in **Eqn (1)** is reminiscent of a series combination of resistance and inductance where the resistive part has the numerical value of the parallel inductance that we have been analyzing. Similarly, the imaginary (reactive) component has the numerical value of the parallel resistance. Clearly, we can construct a series combination of R and L (**Figure 1B**) with the same characteristics as the parallel one provided we assign values as follows:

$$X_s = \left[\frac{R_pX_p}{R_p^2 + X_p^2}\right]R_p \quad (2A)$$

$$R_s = \left[\frac{R_pX_p}{R_p^2 + X_p^2}\right]X_p \quad (2B)$$

where the subscripts "p" and "s" indicate parallel and series components, respectively.

Taking the ratio of these two equations yields:

$$\frac{X_s}{R_s} = \frac{R_p}{X_p} = Q$$

from which **Eqns (2A)** and **(2B)** can be manipulated to yield:

$$R_p = R_s\left(1 + Q^2\right) \quad (3A)$$

$$X_p = X_s\left(1 + 1/Q^2\right) \quad (3B)$$

which are the familiar impedance-matching equations.

We see immediately that the common term in [brackets] in **Eqns (2A)** and **(2B)** is a scaling factor relating parallel to series equivalent as can be shown in a diagram of **Figure 2**, which demonstrates the validity of Eric Nichols' Figure 4.

Since, from **Eqns (2A)** and **(2B)**, R_s is proportional to X_p, and X_s is proportional to

(Continued on page 24.)

John M. Franke, WA4WDL
4500 Ibis Ct., Portsmouth, VA 23703 | **jmfranke@cox.net**

Precision Blocks for Machining Waveguides and Matching Circuits

Repurposed waveguide sections serve as drilling guides.

Accurately and securely holding sections of waveguide while drilling, cutting or sanding can be difficult, particularly when flanges are attached to the waveguides. The problem can be overcome by using what would otherwise end up as scrap metal. In this case I repurpose waveguide circulator blocks. The blocks have three important features. First, three primary faces are already drilled and even sometimes threaded, for standard broadband waveguide flange layout patterns and screw holes. Second, the faces are mutually perpendicular. Third, the blocks are much cheaper than buying precision ground machinist blocks. My intent was to take advantage of the precision machining already done by the original manufacturer.

Not all waveguide circulators are usable. I am always on the lookout for ones machined to tight mechanical tolerances and if tuned, for frequencies not used for amateur radio work. After all, it would be wasteful to modify circulators having resonant cavities and ferrite structures covering the 3 cm amateur radio band and/or in my case popular civil and military aircraft and marine radar frequencies. I am primarily interested in three main sizes, WR75, WR90, and WR112. Most useful are circulator blocks with standard flange patterns and holes.

Figure 1 shows five examples of circulators I have used; two WR75, two WR90, and one WR112. The two WR75 circulators, labeled 1 and 2, are narrowband and tuned for commercial satellite television downlinks and commercial digital link frequencies. The WR90 and WR112 circulators, labeled 3, 4, and 5, were intended for use on civil and military radar frequencies. Currently, I am on the lookout for a WR284 circulator.

The circulators are easily checked for "squareness" using a machinist or carpenter try square. An alternate test is to simply slide pairs of circulators together on a common flat surface. The faces should all meet with no significant gaps. Once accepted, the circulator can be clamped in a drill press vice and extraneous material removed using an appropriate size drill or mill bit.

Attaching waveguide sections to the blocks is easy, see **Figure 2**. With the waveguide sections mounted, it is easy to clamp or hold everything in position for accurate machining. The flanges also serve as accurate hole layout guides. **Figure 3** also shows a section of WR90 waveguide attached to a circulator having a flat stabilizer plate, which was added to facilitate bolting on a drill press stage or sliding

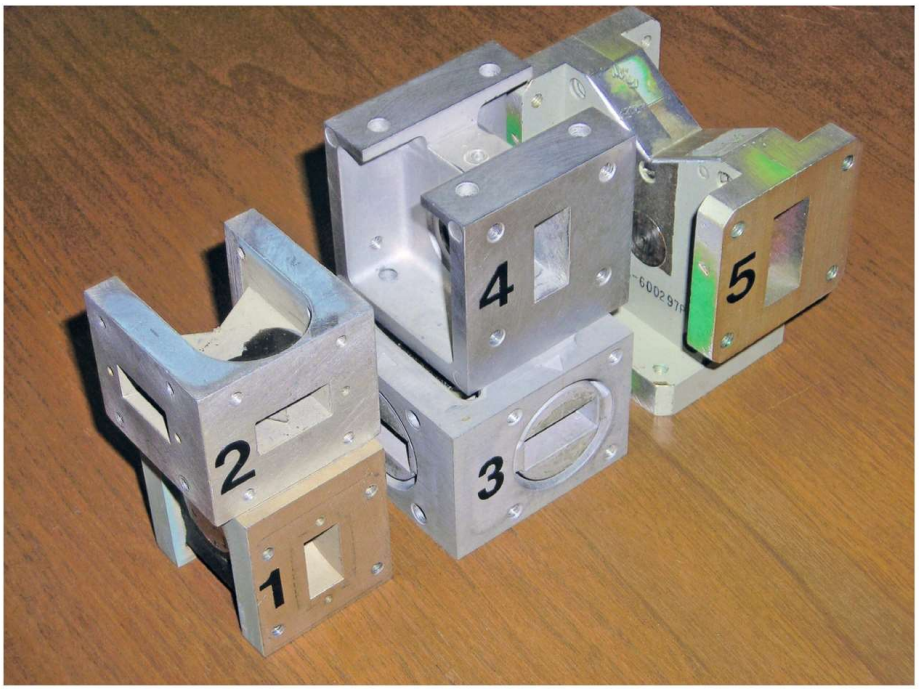

Figure 1 — WR75 circulators labeled 1 and 2 are for commercial satellite television downlinks and digital links. The WR90 and WR112 circulators, labeled 3, 4, and 5, were intended for use on radars.

Figure 2 — Clamping or holding everything in position for accurate machining is easy. Flanges can serve as accurate layout guides.

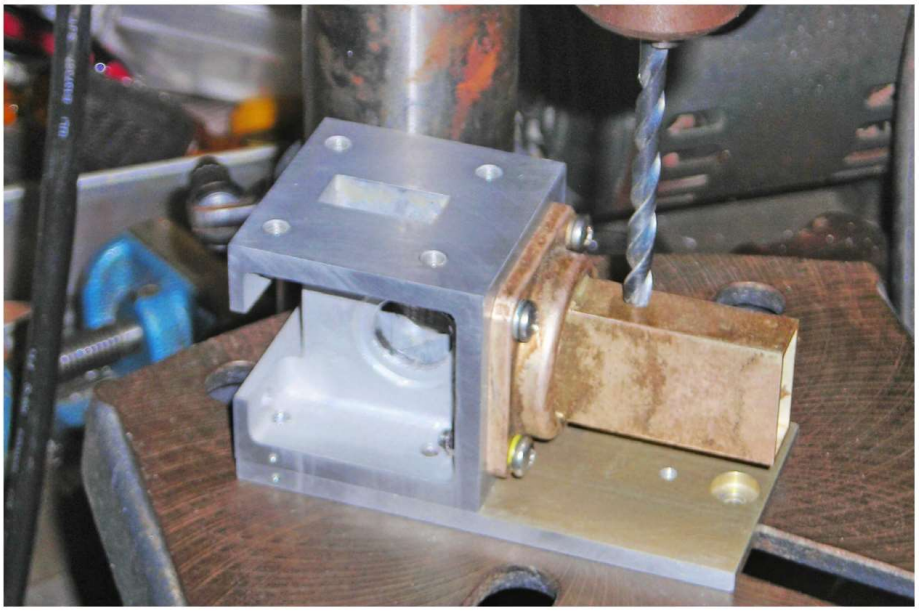

Figure 3 — A section of WR90 waveguide attached to a circulator having a flat stabilizer plate facilitates bolting to a drill press stage or sliding about on a work table. The multiple, mutually perpendicular faces, makes it easy to position a block to present the most desired orientation for drilling, marking or machining.

about on a disc sander work table. With the multiple, mutually perpendicular faces, it is easy to position a block to present the most desired orientation for drilling, marking or machining.

John M. Franke, WA4WDL, earned a Novice license in the mid-sixties. and currently holds an Amateur Extra license, WA4WDL. He also holds a General Radiotelephone Operator License, with Ship Radar Endorsement. He used the license to work through college as a transmitter engineer at two AM broadcast stations. John's degrees include AAS, BSEE and MS, in physics. He retired from NASA in 2005 after more than 30 years. He also served as a radar operator onboard E-2B Hawkeye aircraft in the Naval Reserves. John was a member of the Association of Old Crows for over 25 years. Interests include electronic warfare, microwaves, VLF, and precision timing. He is an inventor or co-inventor on three US patents. John has authored or co-authored 130 professional and amateur radio publications.

(Continued from page 22.)

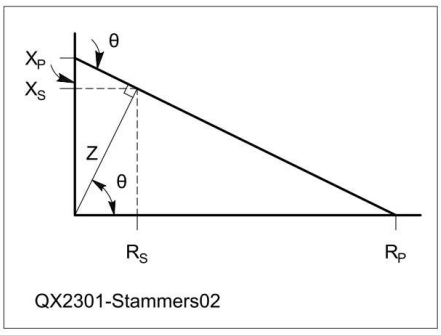

Figure 2 — Shown is the relationships between the series and parallel element magnitudes. The magnitude of the impedance is the same for both parallel and equivalent series forms, and the impedance vector is perpendicular to the $X_p - R_p$ line. The phase angle is shown.

R_p (with the same scaling factor) the impedance vector is necessarily perpendicular to the X_p-R_p line as shown in Eric's Figure 4.

Note in particular that the ratio

$$\frac{R_p}{X_p} = \frac{X_s}{R_s} = \tan(\theta)$$

as before, and will be negative for a capacitive reactance.

As Eric implies, with the advent of hand calculators the use of the graphical solution is probably of historical interest only, but a glance at **Figure 2** shows that one can convert quickly between series and parallel resistance/reactance — for example when impedance matching — and measure quickly the impedance of the combination by drawing the perpendicular from the hypotenuse to the origin. The figure shows also that the phase angles for the parallel and equivalent series arrangements must be the same, by similar triangles. One still needs to calculate the reactance from the value of the reactive element (and vice versa) but many people will have such conversion routines already programmed into their smart phone or computer.

Keith Stammers, GØSXG, worked in several research environments until retirement in 2007, including in archaeological dating by thermoluminescence for which he gained an MSc. He also worked in various positions at the UK Atomic Energy Authority. Keith has had a lifelong fascination with wireless communication, and has dabbled in the theory and experiment of basic RF electronics. He is a member of the Institute of Physics and the Society for Radiological Protection.

H. Scott Lentz, AG7FF
511 E. 5th St., Libby, MT 59923 | **scott.ag7ff@gmail.com**

The Lentz Receiver: Tayloe Evolved

This design is purpose-built to provide high image rejection.

In an effort to design my own pocket-sized transceiver, I've been working with different receiver designs for a couple years now, and I'm ready to share my latest design. Unlike current direct-conversion receivers utilizing "Tayloe Detectors," this design is purpose-built for high image rejection of >70 dB, see **Figure 1**, with a low MDS (minimum discernible signal) sensitivity across all the HF bands, **Figure 2**. Technically, my receiver design can be characterized as a direct-conversion receiver (i.e., homodyne, first developed in 1932). It uses Hartley **[1]** image rejection architecture and builds on the work of Tayloe **[2]** and Campbell **[3]**. There are three new things here: 1) a method of sampling I and Q that is slightly different from Tayloe, 2) a finished amplification stage, and 3) the incorporation of a DSP (Digital Signal Processing) integrated circuit for the phase shifting to perform image cancelation as suggested by Campbell and Youngblood **[4]**.

Before going into the specifics, let's take a step back and review why image rejection matters. With a direct-conversion receiver, there is no IF (intermediate frequency) – the oscillator in the receiver operates at or near the frequency of interest. So for example, if you want to receive a CW transmission at 14.100 MHz with a 500 Hz tone, you would program (or tune) your oscillator to 500 Hz below that frequency, i.e. 14.099500 MHz. Unfortunately, with a direct-conversion receiver, the problem comes from transmissions that are 500 Hz below your oscillator frequency, at 14.099000 MHz. Commonly called the opposite sideband, it is technically also the undesired image in a direct-conversion receiver, and without image rejection, you receive this signal just as strongly as the frequency of interest. For CW operations, this can result in confusing the receive frequency and then transmitting back a kilohertz or more away from whom you're trying to QSO.

How does image rejection help? When I say that there is >70 dB of image rejection with this new receiver design, it means that the signal of the image must be >70 dB, or 10 million times, stronger than the desired frequency to have the same

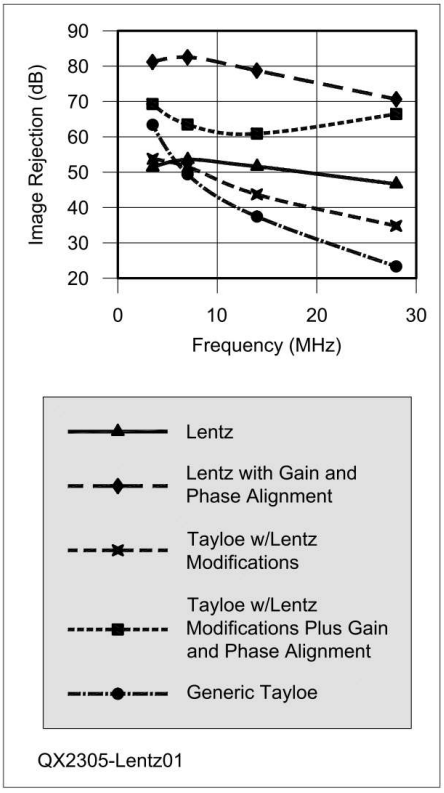

Figure 1 — Image rejection of the Lentz and modified Tayloe receivers using either (a) DSP with a simple Hilbert Transform of 90° for image rejection, or (b) DSP precision phase and gain alignment for image rejection. Higher values are better.

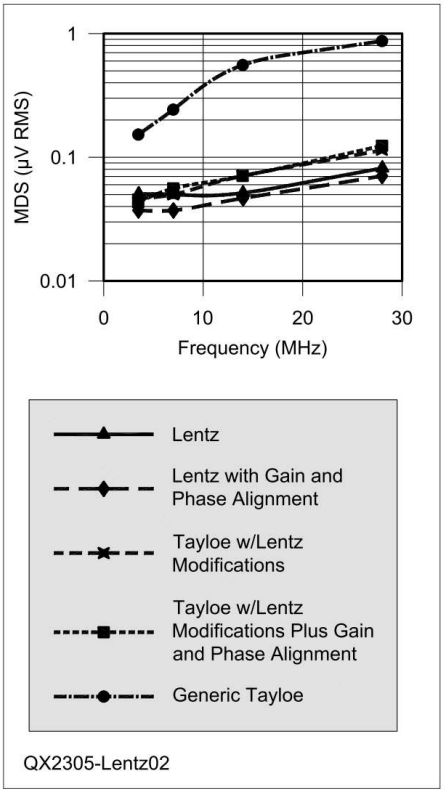

Figure 2 — The minimum discernible signal by frequency using the ARRL's 3 dB-over-noise CW method with a 500 Hz filter. Lower values are better.

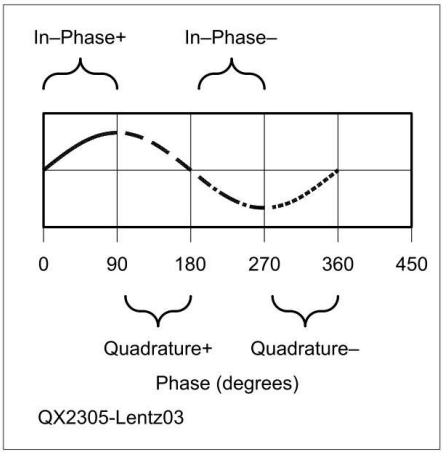

Figure 3 — The 90° sampling of a Tayloe detector.

signal strength as the desired signal. This amount of image rejection is similar to superheterodyne receivers that are much more complex; see the specifications for the popular Yaesu FT-991A.

How does image rejection work? Put simply, you sample or mix your received signal with in-phase and quadrature clocks, typically just called I-Q. The quadrature clock is delayed 90°, or in other words, one-fourth the time period of the frequency of interest. Now that we have sampled I and Q, we have baseband (audio) in two channels, which are also 90° shifted. By post-sample shifting (delaying) the audio quadrature channel another 90° and adding the signals back together, the signals either double (for the desired signal, i.e. the proper sideband), or the signals cancel (if the image, i.e. the wrong sideband). One way that has been common to do the phase shift is with operational amplifiers using tuned phase delays — see Campbell **[3]** and also the QCX line of transceivers by QRP Labs. Youngblood **[4]** proposed some complex PC based manipulation, but modern DSP integrated circuits allow us to simply add a single design block called a Hilbert Transform, which will do the 90° rotation for us. As described later, we will do some fine tuning of the phase and gain, but we'll use DSP for that too.

Now that you know the final trick, let's walk through the design to see how I optimized for it. I spent two years working with the Tayloe detector with which most of you will already be familiar. The Tayloe detector is an I-Q sampler patented more than 20 years ago and is included in the current *ARRL Handbook*. Tayloe functions by chopping the incoming signal at the receive frequency into four segments with a multiplexer, see **Figure 3**. In other words, it takes 90° samples of the incoming RF wave, and stores the sampled voltage in capacitors before forwarding the differences on to amplifiers, either operation amplifiers, like OpAmps, or instrumentation amplifiers, like InAmps. Using a generic Tayloe design and a 90° Hilbert Transform, I get 60 dB of image rejection at 3.5 MHz, but rejection drops off to only about 25 dB at 28 MHz. Again, see **Figure 1**.

I realized that what I really needed was to have better phase and gain matching between I and Q. I can't emphasize this enough. Phase matching and gain matching are the keys to success here. If you do something that influences either of those, you must control the error it induces, with higher precision components.

In my attempts to optimize for image rejection, I have made several modifications to the Tayloe detector. The results of these are shown as "Tayloe with Lentz modifications" in **Figures 1** and **2**. Note that the "Generic Tayloe" is for general reference only — these results are from an earlier experiment of mine, which does not contain any of the "Lentz modifications" nor the INA849 InAmp. Your results may vary.

1) – I do not bias the receive signal. Because I felt that adding a source of common-mode noise into the signal was counter-productive, I used a capacitively-coupled RF signal throughout the design.

2) – In his example circuit, Tayloe uses four relatively large (0.22 µF) sampling capacitors that are each connected to ground. Unfortunately, I found that I get a significant dc offset on my sampling capacitors with this configuration, especially at higher HF frequencies (>14 MHz). I'm not sure if this is due to charge injection pumping from the multiplexer, but it definitely occurs. Further, I found that mismatching of capacitors leads to larger phase errors, especially at the higher values recommended by Tayloe. The fix here is to cross-connect *one* capacitor *between* the positive and negative samples instead of using *two* to ground for each signal path (I or Q). Reducing the number of capacitors from four to two increases stability of the amplifier and reduces this source of phase and gain errors.

3) – I reduced the value of the capacitors considerably. I found that I got flattest performance in MDS across the HF bands, and best stability of the InAmps, with a cross-connected capacitor of only 100 to 1,000 pF. By using 1% C0G rated caps, you don't have to worry about heat from your transmitter throwing the receiver out of alignment.

This is the point where we are ready to amplify the signals, and where Tayloe's design ends its specifications. To finish the design:

1) – We need to match the gain between the two signals, and this is where InAmps are better than OpAmps. Unlike OpAmps, InAmps require only a *single* resistor to set their gain, and by selecting high precision (0.1%) resistors with low temperature coefficients (25 ppm/°C or less), we can get high gain *and* very good gain matching between the two channels. I have had the most success with one particular low-noise, high-speed InAmp, the Texas Instrument INA849. The Analog Devices version of this, the AD8429, might be a suitable alternative, but I haven't tried it yet. I've successfully pushed the INA849 to provide 1000 V/V gain, so you get 1 mV out from 1 µV in up to 30 MHz. With the INA849, only one chip is required for each signal chain (in-phase and quadrature), and no other hardware amplification is required. Since digital decimation filters are built in to the DSP chip low-pass filters aren't needed; just feed the outputs through dc-blocking capacitors into the DSP ADC (Analog to Digital Converter) inputs. Other InAmps I've tried worked fine at lower frequencies or lower gains. If you use a different InAmp, you'll know when the gain is too high because the output of one or both of the InAmps gets pegged to a power rail, e.g. 4 V or –4 V, in my case.

2) – As required by the InAmp datasheet, I experimented with various current-return resistors and determined that very low values of 50 to 100 Ω on the InAmp inputs worked best to prevent high noise floors.

3) – I used an easily programmed DSP

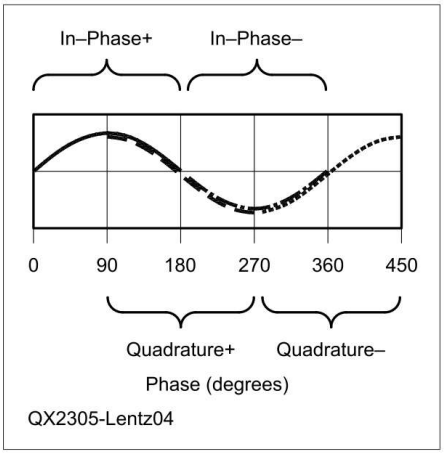

Figure 4 — The 180° sampling of the Lentz receiver.

chip, the Analog Devices ADAU1761, because it comes with the free Sigma Studio graphical programming interface (which also helps author the final C-code for a microcontroller) and because it comes with Hilbert Transform as a built-in design block. Analog Devices has other DSP chips that do the same thing if you search on "Audio Codecs" on their website.

At this point in the modifications, with only hardware changes and a simple 90° DSP Hilbert Transform rotation on the quadrature channel, image rejection is in the 35 to 55 dB range, see **Figure 1**, and MDS is greatly improved compared to my previous experiments with Tayloe, see **Figure 2**. Using further DSP programming for gain (i.e. balance) and phase alignment, I was able to push the image rejection up to 60 to 70 dB, again, see **Figure 1**. This amount of rejection (60 to 70 dB) is pretty good, but my goal was to match a superheterodyne with >70 dB of rejection.

So, I took a step back and, inspired by Campbell **[3]**, I redesigned the Tayloe sampling scheme. Personally, I think that with this new scheme and all my modifications combined, the end result is different enough to warrant a distinct name. This is the Lentz Receiver. Through experimentation, I took what I've already described to improve Tayloe, and then determined that I could get better phase matching and better MDS by splitting the incoming RF signal in half using a simple "Y" in the PCB traces and sampling I and Q separately. Campbell had used a 50 Ω power splitter for this purpose, but a simple Y in the circuit board traces along with 4x100 Ω current-return resistors on the InAmp inputs, two of which are exposed to the incoming signal at any one time, leads to a 50 Ω match to the coax.

Like Tayloe, I chop the signal up and store-and-forward the differential results in capacitors — yes, I tried removing the capacitors completely — but instead of taking a single signal and cutting it into fourths with a 1x4 multiplexer, see **Figure 3**, I use two clocks and two 1x2 analog switches — one precisely delayed by 90° — and cut each signal into halves, see **Figure 4**. This means I'm sampling 180° of the in-phase signal, which is forwarded to the amplifier positive input, and then I'm sampling the next 180° of the in-phase signal (the negative half), which is forwarded to the amplifier negative input. The same thing happens with the quadrature signal chain, except that it is sampled 90° out of phase compared to the in-phase clock. I fully expected my MDS level to be 3 dB worse with this split, but tests showed this design was more sensitive than my best modifications of Tayloe, see **Figure 2**, presumably due to the longer sample time.

One additional change from earlier designs, I had used two CMOS clocks to control the multiplexer. One at the frequency of interest, and one at two times that frequency, in order to match the truth table of the multiplexer. In my current design, I conditioned the clocks with flip-flops because I found a small technical specification in the oscillator chip datasheet that explained some of the phase error I was getting: "Duty Cycle 48 – 52%." In other words, the CMOS clock output wasn't guaranteed to be a symmetrical square wave, it was only guaranteed for the rising edge. So, like several people

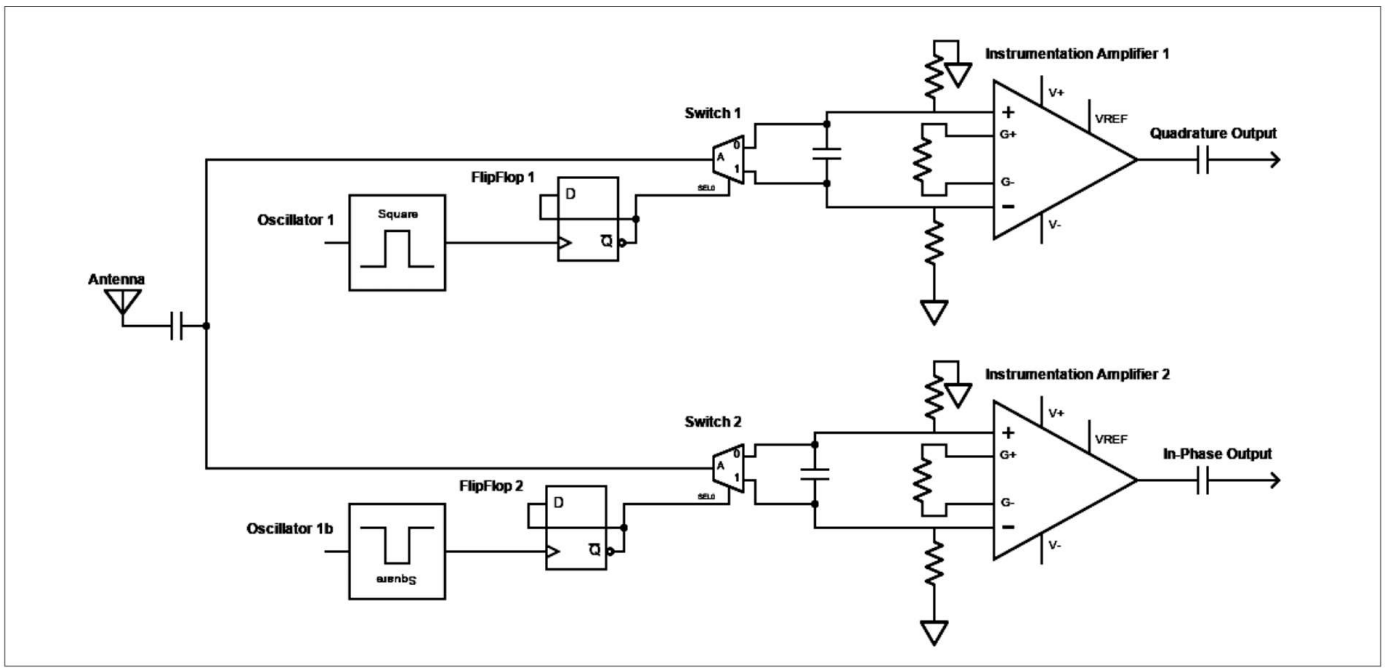

Figure 5 — The basic design of the Lentz receiver minus the power supply tree. Oscillator 1b is the complement, or inverse, of Oscillator 1. The two flip-flops are rising edge triggered.

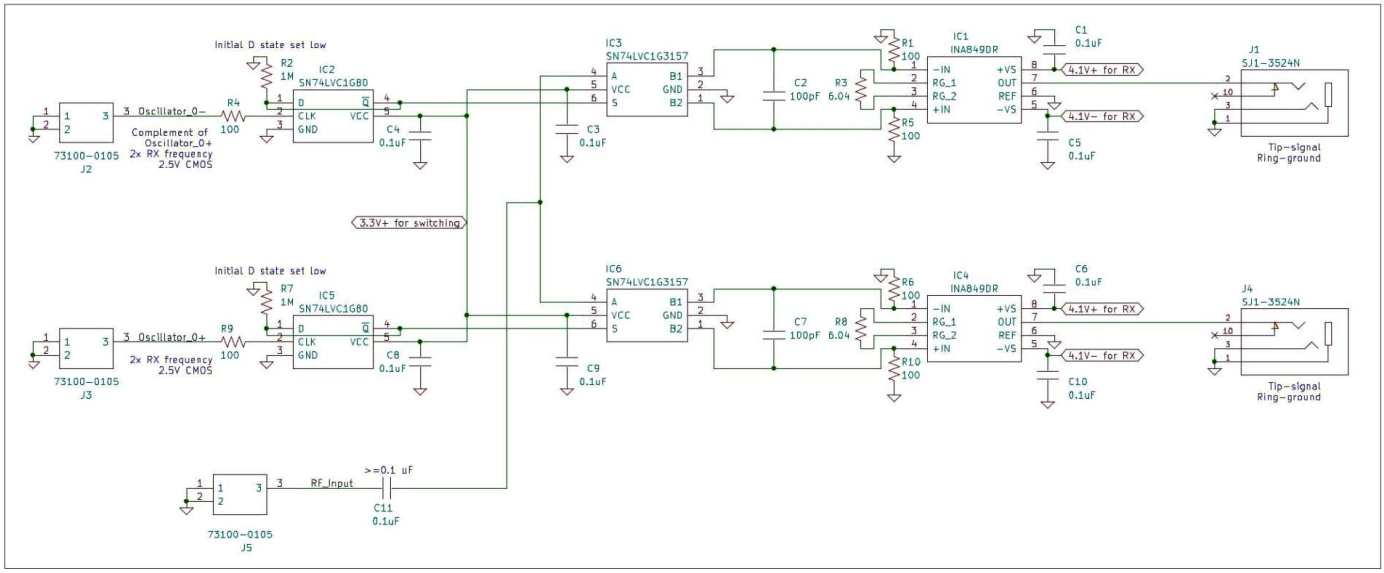

Figure 6 — Specific part selection and connections that I used for the Lentz Receiver in all tests.

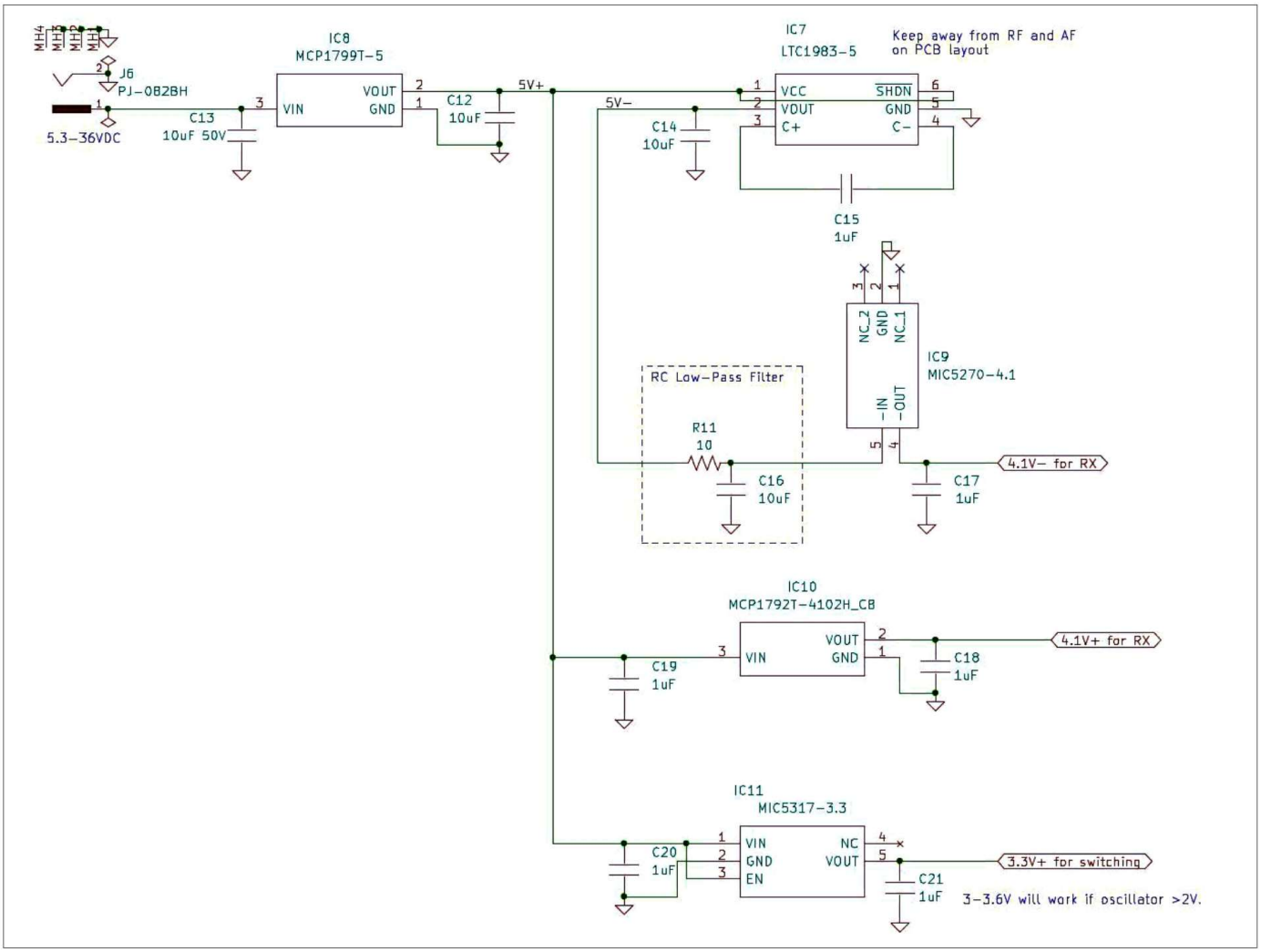

Figure 7 — The simplest power tree that I have come up with. Without the oscillator board or DSP board, the receiver draws 40 mA.

have already published online, I selected flip-flops that are rising-edge triggered to create the square wave CMOS clock needed at the two analog switches. As usual, to get a given frequency out of the flip-flop, the oscillator chip operates at two times the receive frequency and every rising edge of the clock represents a change from low-to-high or high-to-low CMOS level output from the flip-flop. For the quadrature clocking, fortunately, the oscillator chip I chose, the Skyworks Solutions Si5340D **[5]**, can provide "complementary" clocks (180° out of phase on its rising edge) from a single programmed output. Because I'm already operating at twice the receive frequency, the base clock and the complementary clock combine for four times the receive frequency to equal a quadrature clock. So the complementary clock gets its own flip-flop and analog switch, and the two signals are 90° out of phase. This is simple and a much more precise phase shift than using the CMOS outputs of the Si5340D directly.

If you build the clock section and use the flip-flops that I did (without set/reset), add a high value (1 M Ω) resistor from the flip-flop D to ground, and then for proper startup: 1: Switch on the power to the oscillator first and "disable" but don't "power down" the clock, 2: Switch on the power to the flip-flops (and to the rest of the board is okay too), and only then, 3: Enable the clock. This ensures that the flip-flops are properly initialized so that you always get the same sideband when you turn it on. After turning the clock on this way, you can manipulate the clock frequency without fear of selecting the alternate sideband because this clock IC has zero-crossing frequency changes (which also means, say good-bye to those annoying clicks when changing frequency!).

The end result is the design shown in simplified form in **Figure 5**, and completed schematics with the specific parts shown in **Figures 6** for the receiver signal chain, and **Figure 7** for the power tree. Note that the DSP and oscillator sections are not displayed because I used manufacturer-provided development boards. Please refer to the datasheets for those products to determine the ancillary components for a complete and final receiver design.

Without specific phase and gain alignment, just a simple 90º Hilbert Transform, I get 45 to 55 dB of image rejection and MDS levels — using ARRL's CW method,

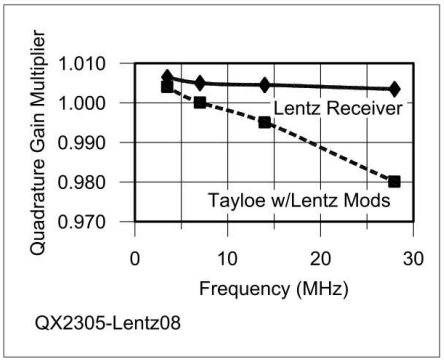

Figure 8 — The amount of gain applied to the quadrature channel to balance with the in-phase channel for the maximum image rejection values displayed in Figure 1 for the "Tayloe with Lentz modifications" and for the Lentz Receiver. The flatter line is better.

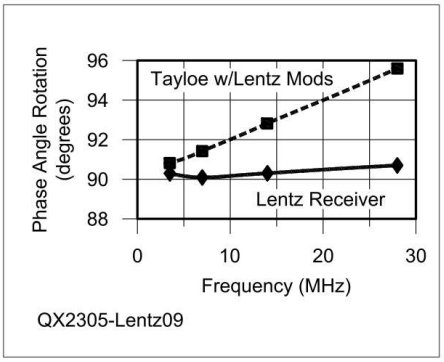

Figure 9 — The amount of phase rotation applied to the quadrature channel before adding to the in-phase channel for the maximum image rejection values displayed in Figure 1 for the "Tayloe with Lentz modifications" and for the Lentz Receiver. The flatter line is better.

which is 3 dB rms over noise with a 500 Hz filter — of around 0.05 to 0.08 μV rms at 50 Ω (–133 dBm to –129 dBm).

My testing method mimics the ARRL Lab. I use a Behringer UCA202 line level USB interface between the DSP headphone output and a laptop running True Audio TrueRTA Audio Spectrum Analyzer Level 4 Software. The RF signal is generated with a Siglent SDG1032x arbitrary waveform generator set for 50 Ω output of sine waves measured in rms voltage output levels in the low millivolt range. The generator has an SDR-Kits Mini Low-Jitter Precision GPSDO Reference Oscillator connected to it for accuracy. A 50 Ω cable connects to the antenna port of the receiver board through several 50 Ω RF fixed attenuators that sum to either –40 dB, –70 dB, or –100 dB. I turn on the radio under test, set the DSP for 500 Hz-wide filtering centered on 500 Hz (my preferred sidetone). I also use a peaking filter and headphone amplifier in the DSP, which adds 15 dB and 6 dB respectively to the gain of the InAmp in these measurements. Without any input signal, I record the rms dBm of the noise level shown in the software. I then turn on the signal generator and adjust the signal for approximately 3 to 4 dB higher rms to determine the MDS. I say approximately because these levels fluctuate with the noise up to about ±0.5 dB, and my measurements are conservative, which means I make sure there is at least 3 dB difference. Next, I retune the signal generator to 500 Hz below the oscillator for the image (and usually remove 30 dB or 60 dB of attenuation) then increase voltage on the signal generator until the 500 Hz sound level reads the same value of 3 to 4 dB over noise rms. I record the voltage level of the input in millivolts rms, and do the attenuation and logarithm math in a spreadsheet for the reject level.

With DSP band-specific gain and phase alignment, I get image rejection numbers approximately 25 dB better (70 to 82 dB) and MDS levels a couple hundredths of a microvolt lower (–136 dBm to –130 dBm), see **Figures 1** and **2**. Although you can use DSP gain and phase alignment of I and Q for any quadrature receiver, the Lentz Receiver requires much less alignment than Tayloe (with Lentz modifications) for maximum image rejection, see **Figures 8** and **9**.

So that's all the good stuff; what are the downsides to my design? The biggest drawback is also its biggest benefit. The design obviously requires a DSP chip, which in turn requires software on a microcontroller to program and adjust the DSP. You will also need to write the microcontroller code for the oscillator and probably a display, but with a modern radio, you are probably doing this already. This is a software intensive design; one that some would call a "software defined radio." I'm at the stage where I've finished the receiver design using development boards from the manufacturers for the oscillator and DSP chips plugged into a laptop to control them over USB (that's the bus not the sideband) using manufacturer provided graphical interfaces. I've spent two years getting to this point, and I'll probably spend a month on the C-code software for a microcon-

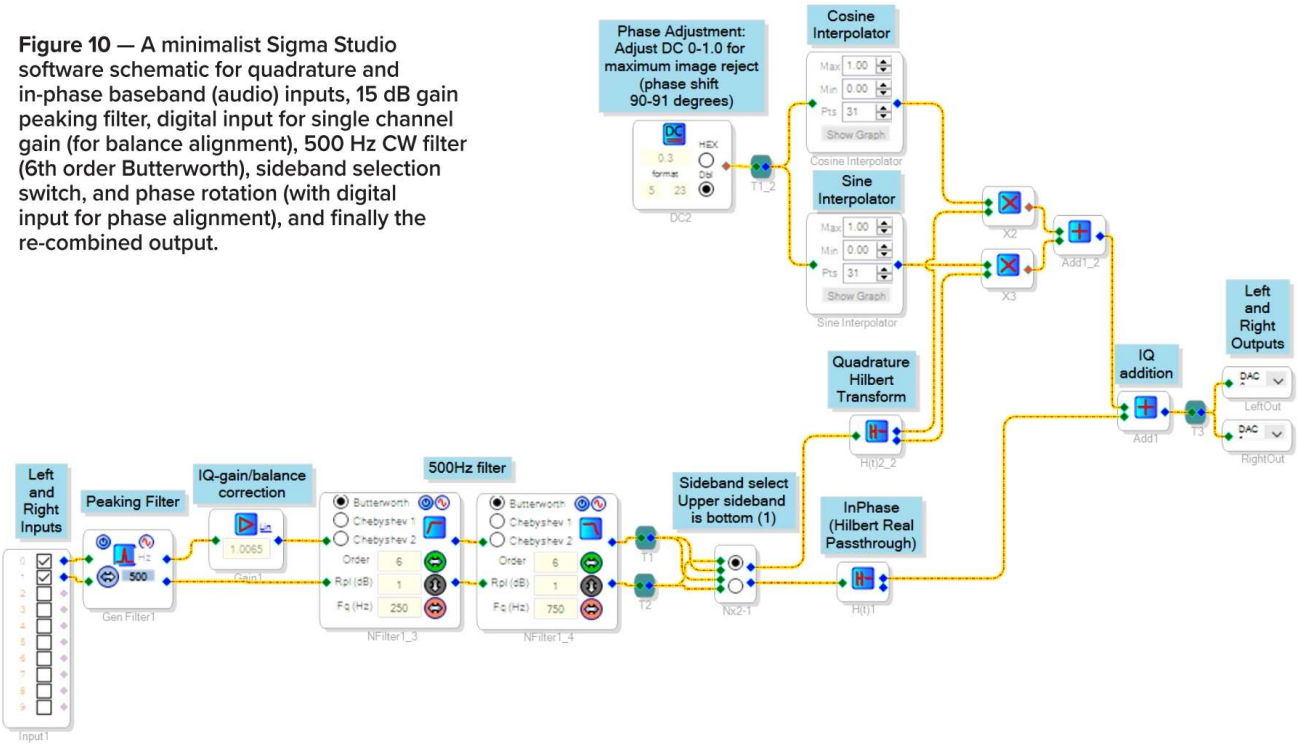

Figure 10 — A minimalist Sigma Studio software schematic for quadrature and in-phase baseband (audio) inputs, 15 dB gain peaking filter, digital input for single channel gain (for balance alignment), 500 Hz CW filter (6th order Butterworth), sideband selection switch, and phase rotation (with digital input for phase alignment), and finally the re-combined output.

troller to control and display my final transceiver design.

Note that whether you incorporate some or all of my modifications, or adopt my final design, I want to make it clear that I have no interest in patenting these developments. I intend them to be "Open Source Hardware" for the good of all, and upon receipt by the public of this article, should be considered "prior art."

Here are a few more notes that I'd like to share on programming the DSP chip. Please refer to **Figure 10** for the DSP software schematic, which is also available on the **www.arrl.org/QEXfiles** web page, as a complete Sigma Studio file download to program your DSP chip. If you wish to mimic my simple 90° Hilbert phase shift results without gain and phase alignment (the solid lines in **Figures 1** and **2**), delete the gain block and then simply connect the imaginary output from the quadrature Hilbert Transform block to the I-Q addition block, and skip the sine and cosine table multiplications and addition.

First, a software trick is needed, which is not well documented. In order to get the Hilbert Transform to work correctly for this usage, you need two Hilbert Transform blocks — one that has the input from the in-phase channel and one that has the input from the quadrature channel. For the in-phase channel, you are just passing one channel through the "Real" side to apply the appropriate time delay so that both channels match properly. It won't work if you don't do this.

For phase alignment, the configuration is a bit complex with multiplication by sine and cosine lookup tables on the quadrature output from the Hilbert Transform block, but the actual usage is to enter a single number for phase rotation. I followed the design example published online (**https://ez.analog.com/dsp/sigmadsp/f/q-a/65849/how-to-use-sigmastudio-software-to-realize-an-external-potentiometer-to-control-phase-the-phase-of-the-range-is-0-to-180**), and I modified it to include a dc input block (0 to 1 V in decimal form) instead of a potentiometer and reduced the range of phase adjustment of 90° to 100° degrees for Tayloe or 90° to 91° for the Lentz Receiver. My lookup table multiplier values (31 values each) for the cosine and sine interpolators are shown in **Table 1**, also on the **QEXfiles** web page.

Next for gain (balance) alignment: place a gain block on the quadrature audio line before the Hilbert Transform, and adjust as necessary for maximum image reject. This is a multiplier block, so you set it to 1.0 for no change, or greater than 1.0 for gain on the channel, or less than 1.0 for attenuation of the channel. In tweaking this value with the Lentz Receiver, note that 0.0005 steps actually make a difference.

During my experiments, I found that I needed to go back and forth between phase alignment and gain alignment 2 or 3 times to get the best image rejection for that band. Now that I see the final values graphed (**Figures 8** and **9**), a bit of linear interpolation between the alignment of 7 MHz and 28 MHz will probably get me pretty close to the bands in between, and I may be able to let the microcontroller do the math.

Obviously the DSP chip can do a lot more than just our image rejection. This DSP chip has 2-channel (i.e., stereo) ADCs (Analog to Digital Converters) and DACs (Digital to Analog Converters) built in. It has a headphone amplifier, greatly simplifying output circuitry. In software we can swap the input channels to select upper or lower sideband by swapping which channels get the quadrature processing. We can easily create a very helpful peaking filter. We can drop in a 3000 Hz voice filter, or a 500 Hz CW filter or narrow it down even further. Obviously, we have attenuation and volume control, etc.

Looking ahead, I'm sure it is only a matter of time until some company releases a flip-flop or clock buffer that

Table 1 – Lookup table multiplier values for the cosine and sine interpolators.

Degrees	Cosine lookup	Sine lookup
90.00000	0.000000000	1.000000000
90.03333	-0.000581776	0.999999831
90.06667	-0.001163553	0.999999323
90.10000	-0.001745328	0.999998477
90.13333	-0.002327104	0.999997292
90.16667	-0.002908878	0.999995769
90.20000	-0.003490651	0.999993908
90.23333	-0.004072424	0.999991708
90.26667	-0.004654195	0.999989169
90.30000	-0.005235964	0.999986292
90.33333	-0.005817731	0.999983077
90.36667	-0.006399497	0.999979523
90.40000	-0.006981260	0.999975631
90.43333	-0.007563021	0.999971400
90.46667	-0.008144780	0.999966831
90.50000	-0.008726535	0.999961923
90.53333	-0.009308288	0.999956677
90.56667	-0.009890038	0.999951092
90.60000	-0.010471784	0.999945169
90.63333	-0.011053527	0.999938908
90.66667	-0.011635266	0.999932308
90.70000	-0.012217001	0.999925370
90.73333	-0.012798732	0.999918093
90.76667	-0.013380458	0.999910478
90.80000	-0.013962180	0.999902524
90.83333	-0.014543898	0.999894232
90.86667	-0.015125610	0.999885601
90.90000	-0.015707317	0.999876632
90.93333	-0.016289019	0.999867325
90.96667	-0.016870716	0.999857679
91.00000	-0.017452406	0.999847695

utilizes one of the better differential clocking methods, e.g. LVDS (Low Voltage Differential Signaling) with the CMOS outputs necessary for the analog switch, or even LVDS-controlled analog switches. Better yet, someone will probably release a single quadrature sampling chip that includes the oscillator and switches. Also, watch the market for even lower noise, high-speed InAmps and DSP chips with more memory and MIPS than currently produced.

Software

FINAL_DSP_program_for_Lentz_Receiver_article.dsppproj is the DSP software needed by the Lentz Receiver. It is available from **www.arrl.org/QEXfiles** web page, and requires the user to download and install the free SigmaStudio software from Analog Designs in order to program their DSP development board.

H. Scott Lentz, AG7FF, holds an Amateur Extra class license. He was first licensed in 2003. His ham radio interests shift every few years, and most recently he has been working on designing a CW transceiver from scratch. Scott retired early from the US Forest Service where he was a fisheries biologist for his regular job and a communications technician for his fire job. He holds a BS in Aquatic Wildlife Biology and an MS in Organismal Biology and Ecology, both from the University of Montana.

Notes

[1] R. Hartley, "Modulation System," US patent 1,666,206, 1928.

[2] D. Tayloe, "Product detector and method therefore," US patent 6,230,000, 1998.

[3] Campbell, R. KK7B, "High-Performance, Single-Signal Direct-Conversion Receivers," *QST* Jan. 1993, pp. 32-40.

[4] G. Youngblood, AC5OG, "A software-defined radio for the masses, Part 1," *QEX* July/Aug., 2002, pp. 13-21.

[5] The oscillator development board comes with capacitive coupling of the clocks. These capacitors must be removed and replaced with 0604 sized resistors or jumpers to use the CMOS clocks. See the development board datasheet for more information.

Errata

- In S. Geers, KA8BUW, "DSP CW Filter," *QEX* Jan./Feb. 2023, in Figure 1 the + and – inputs on op-amps U1 and U2 should be reversed. Thanks to Bob Liesenfeld, WBØPOQ, for pointing out the error.
- In Dr. U. L. Rohde, N1UL, "AM and FM Noise in Oscillators," *QEX* Mar./Apr. 2023, p. 5, Eqn (8-11) should be:

$$L\frac{di(t)}{dt}+\left(R_L-R_N(t)\right)i(t)+\frac{1}{C}\int i(t)dt=e_N(t)$$

Thanks to James McNamee, KEØNRE, for spotting the error.

Dr. Philip Cassady, K7PEC
40106 SE 60th St., Snoqualmie, WA 98065 | **philipcassady@centurytel.net**

Addendum to Tuned Transformer *QEX* Article

The recently published tuned transformer performance is clarified and improved.

Clarifications and improvements of the end-fed half-wave antenna tuned transformer performance that was recently published in *QEX* are presented. The reduced SWR afforded by the presence of a parallel primary capacitor is affirmed using a more realistic circuit analysis.

Gerald Julien Lemay, VA2GJ, published a very interesting and informative article **[1]** in the July/August 2022 *QEX* magazine in which he described how the SWR performance of an end-fed half-wave antenna can be improved by the addition of a capacitor parallel to the impedance transformer primary winding. The Lemay article clearly describes the operation of such a tuned transformer and provides performance equations. However, several steps of the derivation were not included, and the final equations for the SWR were not printed correctly.

The correct expressions for the final SWR equations will be presented in this addendum. In addition, the theoretical description of the tuned transformer operation will be improved and a more realistic calculation of the SWR performance will be presented.

In his *QEX* article, Lemay presents a thorough and very clear explanation of the tuned transformer operation. His performance equations through his Eqn (10) are well developed and easily understood. The difficulties appear with his definition of SWR and his subsequent Eqns (11) and (12). Following his derivations, the corrected version of his Eqn (11) should read:

$$\left|\mathrm{SWR}\right|_{without\ C} = \frac{Z_0}{\alpha Z_L} = \frac{Z_0}{Z_L}\frac{N_S^2}{N_P^2}\sqrt{\left(\frac{N_P}{N_S}\frac{V_P}{I_s \omega L_P}\right)^2 + 1}$$

the corrected version of his Eqn (12) should read:

$$\left|\mathrm{SWR}\right|_{with\ C} = \frac{Z_0}{\alpha Z_L} = \frac{Z_0}{Z_L}\frac{N_S^2}{N_P^2}\sqrt{\left(\frac{N_P}{N_S}\frac{V_P\left(1-\omega^2 L_P C_1\right)}{I_s \omega L_P}\right)^2 + 1}$$

All equation numbers refer to equation numbers in the original Lemay **[1]** article. These equations are correctly plotted in Figure 4 of **[1]** using the parameters:

$C_1 = 150$ pF, $Z_0 = 50\ \Omega$, $Z_L = 3200\ \Omega$, $V_P = 50\ \mu$V, $N_P = 3$, $N_S = 24$, $I_P = 1\ \mu$A

At a resonant frequency of 14 MHz the inductance of the transformer primary is given as $L_P = 0.8616\ \mu$H.

The current in the transformer secondary is calculated from the transformer equation:

$$I_s = I_p \frac{N_P}{N_s} = 0.125\mu\mathrm{A}$$

However, Eqn (5) states that (using sL_p=Z):

$$I_P = \frac{V_P}{sL_P} + \frac{N_s}{N_P} I_s = \frac{V_P}{Z} + \frac{N_s}{N_P} I_s$$

The first term on the right hand side, the primary circuit magnetizing current, has been neglected in the Tuned Transformer article **[1]**. It is straightforward enough to include the primary circuit magnetizing current using the equations presented in **[1]**.

In order to determine the SWR, we need to calculate the impedance mismatch between the transformer primary, Z_P , and the transmission line, Z_0. Z_P can be calculated using the equations presented in **[1]** as Eqn (8),

$$Z_P = \alpha Z_L$$

and Eqn (9),

$$\alpha = \frac{N_P / N_s}{\frac{V_P}{I_s Z} + \frac{N_s}{N_P}}$$

leading to Eqn (5) for I_P.

$$I_P = \frac{V_P}{sL_P} + \frac{N_s}{N_P} I_s = \frac{V_P}{Z} + \frac{N_s}{N_P} I_s$$

The first term in the denominator of Eqn (9) can be written as:

$$\frac{V_P}{I_s Z} = \frac{V_P}{I_P Z}\frac{I_P}{I_s} = \frac{Z_P}{Z}\frac{I_P}{I_s}$$

Then Eqn (5) can be used to show that:

$$\frac{I_P}{I_s}=\frac{V_P}{I_s Z}+\frac{N_s}{N_P}=\frac{Z_P}{Z}\frac{I_P}{I_s}+\frac{N_s}{N_P}$$

This equation can be solved for I_P/I_s

$$\frac{I_P}{I_s}=\frac{N_s/N_P}{1-\frac{Z_P}{Z}}$$

which is then substituted into the expression for the first term in the denominator of Eqn (9):

$$\frac{V_P}{I_s Z}=\frac{V_P}{I_P Z}\frac{I_P}{I_s}=\frac{Z_P}{Z}\frac{I_P}{I_s}=\frac{N_s}{N_P}\frac{Z_P}{Z-Z_P}$$

When this is substituted into Eqn (9) we get an equation for α in terms of the impedances and transformer turns ratio:

$$\alpha=\left(\frac{N_P}{N_s}\right)^2\frac{Z-Z_P}{Z}$$

Substituting this expression for α into Eqn (8) yields an expression for Z_P:

$$Z_P=\frac{\left(\frac{N_P}{N_s}\right)^2 ZZ_L}{Z+\left(\frac{N_P}{N_s}\right)^2 Z_L}$$

The impedances are complex functions with both real and imaginary parts:

$$Z_P=R_P+i\,X_P$$
$$Z_L=R_L+i\,X_L$$

Except for the inductor and/or capacitor impedance, which is purely imaginary, and the transmission line impedance, which is purely real:

$$Z=R+iX=iX$$
$$Z_0=R_0+i\,X_0=R_0$$

Complex variable algebra yields the real part (resistance) and imaginary part (reactance) from the above expression for Z_P:

$$R_P=\frac{\left(N_P/N_s\right)^2 X^2 R_L}{\left(N_P/N_s\right)^4\left(R_L^2+X_L^2\right)+2\left(N_P/N_s\right)^2 XX_L+X^2}$$

$$X_P=\frac{\left(N_P/N_s\right)^2 X\left[\left(N_P/N_s\right)^2\left(R_L^2+X_L^2\right)+XX_L\right]}{\left(N_P/N_s\right)^4\left(R_L^2+X_L^2\right)+2\left(N_P/N_s\right)^2 XX_L+X^2}$$

The ARRL Handbook defines the SWR in terms of the magnitude of the reflection coefficient, |ρ| as:

$$SWR=\frac{1+|\rho|}{1-|\rho|}$$

We are interested in the reflection coefficient arising from the impedance mismatch of $Z_p=R_p+iX_p$ and $Z_0=R_0$. *The ARRL Handbook* gives the equation for the magnitude of this reflection coefficient:

$$|\rho|=\sqrt{\frac{\left(R_P-R_0\right)^2+X_P{}^2}{\left(R_P+R_0\right)^2+X_P{}^2}}$$

These equations were used to calculate the SWR for two cases derived in the Tuned Transformer article **[1]**:

1) Without a parallel capacitor $X_{noC}=\omega L_p$

2) With a parallel capacitor

$$X_{withC}=\frac{\omega L_p}{1-\omega^2 L_p C_1}$$

Using several of the same parameters as those used in the Tuned Transformer article **[1]**:

C_1=150 pF, R_0=50 Ω, R_L=3200 Ω, N_P=3, N_s=24, L_P=0.8616 µH

Note that these parameters assume a purely real Load Impedance, X_L=0 considerably simplifying the expressions for R_p and X_p.

Assumptions concerning the voltage and current in the transformer primary winding are not required in this improved analysis which more realistically depends only on the physical parameters of the equipment.

The results are presented in **Figure 1**. These calculations show the benefit of the capacitor, and a higher SWR than those shown in Figure 4 of **[1]**.

The discontinuity in the slope of the lower SWR trace at the resonance frequency of 14 MHz is caused by the lack of resistive damping in the tuned circuit of the transformer primary. Any real transformer primary winding will exhibit resistance as well as inductive reactance. **Figure 2** shows that the inclusion of 5 Ω of series resistance provides damping of the tuned primary circuit and eliminates the slope discontinuity at the resonant 14 MHz frequency.

The coil series resistance for this application is estimated to be less than 0.05 Ω (3 turns of #18 copper wire around a ¼ inch diameter core, including skin effect), so that the primary resistance damping should be negligible, and the SWR performance should follow the solid lower curve. The inductive reactance of the primary winding is 75.8 Ω at 14 MHz.

The most interesting results are shown in **Figure 3**, which

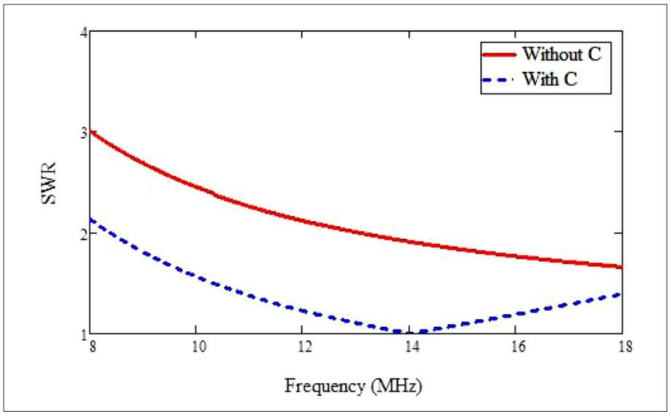

Figure 1 — SWR comparison with and without parallel capacitor over 8 to 18 MHz.

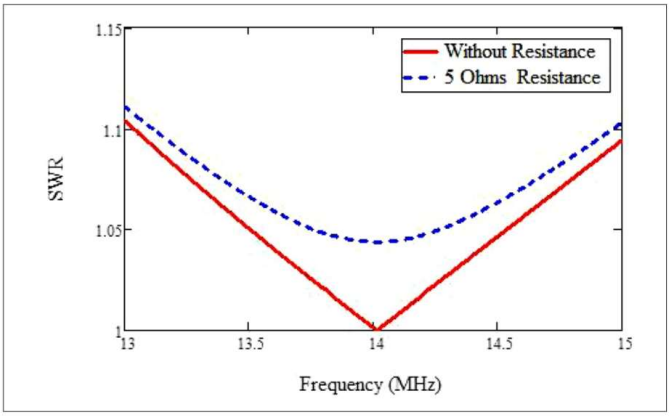

Figure 2 — Resonance with and without resistive damping.

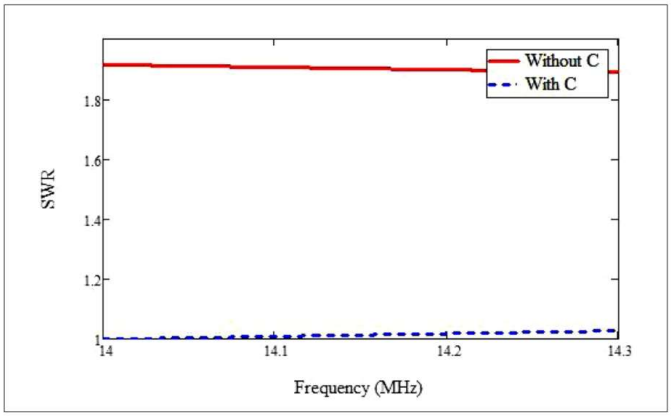

Figure 3 — SWR comparison with and without parallel capacitor in 20 m band.

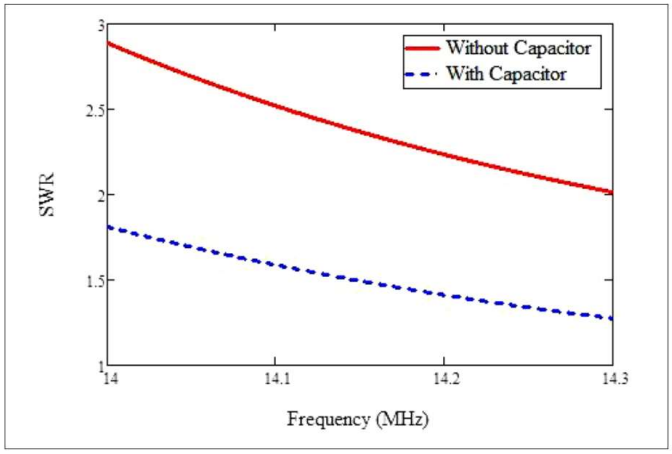

Figure 4 — Reactive antenna SWR with and without capacitor.

shows that the addition of the parallel capacitor reduces the SWR to near 1:1 across the entire 20 meter band.

The impedance of any real antenna exhibits both resistance and reactance. This improved analysis includes the effects of both antenna load resistance and load reactance. The performance of a 20 meter end fed half wave antenna located 30 feet above a real ground was calculated using the 4nec2 computer program. The variations of antenna load resistance and reactance as a function of frequency across the 20 meter band were used as input parameters to calculate SWR. As shown in **Figure 4**, the calculated values of SWR for this reactive antenna were higher than those calculated for a constant antenna resistance without reactance, but the addition of the capacitor is again seen to improve the SWR performance.

Reference

G. J. Lemay, "Tuned Transformer", *QEX* Jul./Aug. 2022, pp. 31-33.

Dr. Phil Cassady, K7PEC, is a retired Boeing Senior Technical Fellow living on a farm with his wife in rural Washington state. He is 82 years old and has been a ham for 10 years, operating only CW mostly on 40 and 80 meters. He is an Amateur Extra class license holder, an ARRL Volunteer Examiner and a member of the Straight Key Century Club. More interested in learning than operating, he has concentrated on antenna design and has constructed four horizontal and two vertical antennas on his farm property. He studied fluid dynamics, plasma physics and lasers at MIT and CalTech, and started in electronics and radio after he retired. Phil is interested in Software Defined Radio, elk hunting and vintage motorcycles.

Eric P. Nichols, KL7AJ
AlasKit Educational and Scientific Resources, 3763 Lyle Ave., North Pole, AK 99705 | **kl7aj72@gmail.com**

Self-Paced Essays – #17 Taking the Lumps Out

Distributed components have physical dimensions that are a significant fraction of the signal wavelength.

Up to this point, in describing electrical circuits, we have dealt exclusively with lumped constants. These are electrical components that are located at a single, physical point in space. One of the assumptions when working with lumped constants is that the speed of electricity is essentially infinite. We know, of course, that electricity does not travel infinitely fast, but in most bench top applications, we can ignore the propagation time of electricity through our circuitry.

When the physical dimensions of a circuit component or components become a significant fraction of the wavelength of the signal that we're working with, we can no longer ignore the propagation time through a circuit.

This brings us to a different way of describing electrical circuits. Rather than describing circuits in terms of discrete components like resistors, capacitors, and inductors at some location, we speak of distributed components. Any length of wire has some amount of self inductance per foot — though generally quite small — and any two conductors near each other exhibit some mutual capacitance.

We trust you have taken the time to view the two film clips suggested in **Essay 16**. The Tektronix clip has a great description of a transmission line being composed of an infinite number of infinitesimal inductances, shunted with an infinite number of infinitesimal capacitances. In such a transmission line we can describe this many-component circuit's behavior in terms of its wave transmission and reflection characteristics.

In fact, and perhaps surprisingly, any electrical circuit can be described by its transmission and reflection characteristics. We've mentioned a few times before that there will always be more than one way of solving any electronics problem, and this is no exception. We can even look at something as simple as a single resistor's transmission and reflection properties and still come out with the right value of resistance or complex impedance!

One of the most wonderful developments in recent years is the arrival of the affordable vector network analyzer, such as the NanoVNA. We will explore the NanoVNA in depth in the next essay, and perhaps in a few subsequent ones.

One term that shows up when speaking of network analysis is scattering parameters, which is really just a formalized way of describing what happens to an electric wave when it encounters a component — either a lumped constant, or something more complex, like a transmission line.

An interesting aspect of distributed circuits is, while with lumped constants we speak of phase shift in terms of time — such as the time difference between voltage and current — with a transmission line or an antenna, we also have to be concerned with phase shift with respect to position. Different things happen at different locations. This will become even clearer when we get to antennas. Just as an introductory comment, a simple wire antenna that's perfectly resonant will have the voltage and current in-phase at any particular location on the wire, but the voltage at one point will not be the same as the voltage at another point. It is this fact what is primarily responsible for an antenna being able to radiate.

But back to transmission lines. It's a good idea to become comfortable with the reciprocals of resistance, reactance, and impedance, namely: conductance, susceptance, and admittance. As a "normal" electronics technician, you can spend most or all of your career without referring to these reciprocal values. In fact, most electronics courses relegate the reciprocals to not much more than a footnote at the end of class. But when working with transmission lines, these will make your life a lot easier. This is why, in my in-person electronics classes, I teach the reciprocals right up front, along with Ohm's Law. Interestingly enough, the power utility folks use the reciprocals a lot more than most electronics techs. This is because power transmission involves the use of many paralleled circuits where the reciprocal values are more convenient.

Now, this is a good time to address the fact that there's nothing magical about "radio frequencies" that make transmission line theory come to life. Our friends at the power company, working with the virtually subterranean frequency of 60 Hz, have to deal with all the distributed component behavior that one has to deal with at microwave frequencies. It's just a matter of degree. To exhibit noticeable transmission line behavior at 60 Hz requires that you have a transmission line tens or hundreds of miles of length but guess what. The power folks do!

Because a transmission line has distributed "components," lengths of transmission lines can indeed be used as substitutes for lumped components. Later on, as we

discuss more of the practical applications of transmission lines, we consider this application a lot more.

Ladder Line to Eternity

Most of the time, when we're working with transmission lines, we actually want the power to do something. Real transmission lines have a finite length, and are normally used to convey power from one location to another. But as we've suggested before, one needs to study the ideal before one dives into the real world. Because of this, it's often useful to explore the infinite length transmission line. The reason for this is that we don't have to contend with reflected power, which always makes things a little more complicated. In the ancient of days in ham radio, the open wire feed line or "ladder line" was the standard type of transmission line. Coaxial cable became available to hams only after World War 2, much to the surprise of most hams born in the 21st Century.

If we look at the input terminals of an infinitely long pair of parallel wires, we would suspect the input resistance (at dc) would read infinity. It is, at first inspection, an open circuit. If we were to take an impedance bridge and just measure the capacitance, we would come up with some finite value of capacitance, which is a function of the diameter of the wires themselves, and the spacing between them. And we would probably assume that we can't actually measure the inductance, because you can't measure the inductance of an open inductor (or even really define it).

With our lumped-constant understanding of the world, we would not normally expect any current to flow into the input terminals of an open transmission line upon applying a dc voltage. But we'd be wrong. In fact — again, assuming an infinite length transmission line — we would find that a finite current will flow. The amount of current that flows will be determined by Ohm's Law. But where is the resistance? It is the "mysterious" entity known as the Characteristic Impedance.

For the general case, one in which there is no resistance, the characteristic impedance of a uniform transmission line, Z_0, is determined by the formula:

$$Z_0 = \sqrt{L/C}$$

Now, obviously, for an infinite length transmission line L and C will also be infinite, so the formula won't make much sense, so we have to qualify those terms as inductance per length, and capacitance per length. And these are things you can actually measure. So now, we can treat Z_0 as a real resistance, and can thus figure out how much current flows.

Here's a little side note to ruminate on. Remember in our "traditional" interpretation of impedance, the reactances (imaginary) values are assigned to energy storage, while resistances (real) are assigned to energy dissipation. In a perfect transmission line, where no energy is dissipated as heat (in other words, no ohmic power loss), Z_0 is a real value, but no energy is dissipated. So we have a lossless real "resistance." How can this be?

Your homework assignment is to come up with a sensible answer to this paradox.

While you're cogitating on this, we'll add a few practical notes.

1) Every type of transmission line, be it open wire feed line, coaxial cable, or microwave waveguide, exhibits the identical behavior in terms of transmission and reflection parameters.

2) For most transmission lines used at low frequencies, most of the power loss is due to I^2R (copper loss) heating. At VHF, UHF, and microwave frequencies, the dielectric losses can become significant, which is one good reason to be comfortable with conductance (G).

3) Transmission lines can be measured at one end (single port) or both ends (two ports), which can both be fully described with scattering parameters. We'll describe this further as we explore the NanoVNA.

4) A properly terminated (matched) transmission line is easiest to analyze, but it isn't always necessary (or even desirable) to use a matched transmission line for many applications.

For a number of historical and practical reasons, 50 Ω is the "default" impedance for coaxial cable. 50 Ω turns out to be a compromise between maximum power handling capacity for a given diameter and minimum loss. Somewhat less common is 75 Ω coax, which has somewhat less loss than 50 Ω, all other things being equal; which they sometimes aren't, which is used primarily for VHF reception. There are also some specialized coaxial cables, mostly for instrumentation, that use characteristics that can diverge widely from those above.

Mr. Smith's Contribution

Whenever the Smith Chart is mentioned, many new technicians, and not a small number of "well-seasoned" engineers tremble with trepidation. We will spend some time taking a lot of the mystery out of the Smith Chart, which contrary to popular opinion, was not invented to make life miserable for hams or other radio folks. Mr. Smith's wonderful chart is much much easier to work with than the hyperbolic trigonometric functions of transmission line formulas that it is based upon. The NanoVNA also helps with understanding the Smith Chart in a way that was not available to us "well-seasoned" folks.

Coming up next time we'll take a close look at the NanoVNA (or even a big VNA, if you have access to one). — *73, Eric.*

Get Ready for Field Day—June 24-25!

Coaxial Cable Assemblies

These low-loss cable assemblies are available in standard lengths with DX Engineering's revolutionary patented PL-259 connector. Use the online Custom Cable Builder at DXEngineering.com to build assemblies made to your exact specs. DX Engineering's coaxial cable is also available by the foot or in bulk spools.
Enter "DXE Assemblies" at DXEngineering.com. From $26.24

DAIWA · Coaxial Dynamics · AMERITRON · Palstar · DIAMOND ANTENNA · Metropwr · ELECRAFT · MONITOR SENSORS

SWR/Wattmeters

Measure forward and reflected transmitter power with SWR/wattmeters from top brands, including Ameritron, Coaxial Dynamics, Daiwa, Diamond, Elecraft, Metropwr, and Monitor Sensors. Choose from models with true peak and average readings, power levels from 20 all the way up to 5,000 watts, amplifier bypass for high SWR, high SWR audio alarms, remote sensors, and more. **Enter "Wattmeter" at DXEngineering.com. From $43.99**

plasticase NANUK PROFESSIONAL PROTECTIVE CASES

RigExpert

RigExpert Analyzer and NANUK Case Combos

In the field, an antenna analyzer is especially at risk for weather and shock damage. We've paired select RigExpert Antenna Analyzers with perfectly sized NANUK equipment cases. Each case is filled with cubed, sectioned foam for custom configuration. Available separately or in combos.
Enter "Analyzer Combo" at DXEngineering.com.
From $382.98

Coaxial Cable Tool Kits

DX ENGINEERING

Get everything you need to prep and install soldered, crimp-on or Universal Compression F-connectors on your coax. For example, the Coaxial Prep Tools for Crimp Connectors Kit (DXE-UT-KIT-CC1) includes cable strippers, grippers, replacement blades, braid trimmer, cable shears and custom hard plastic carrying case. The Ultra-Grip 2 Crimp Connector Hand Tool Kit (DXE-UT-KIT-CRMP2) comes with a ratcheting steel crimper and five die sets for making professional-quality crimps on coaxial and Powerpole® connectors. Individual tools also sold separately. **Enter "Tool Kit" at DXEngineering.com for the full lineup. From $156.99**

Multi-Band Dipole Antenna Kits

DX ENGINEERING

Ideal for easy setup on Field Day, these rugged yet lightweight 2,500W power rated antennas are usable to 30 MHz with a tuner balun (available separately). They feature strong and flexible 14 AWG stranded-copper, relaxed PVC-jacketed elements; 18 AWG 300-ohm ladder feedline; center-T support; and end mount brackets.

DXE-WA-070	Antenna, 70' Long for 40M and Up	**$64.99**
DXE-WA-135	Antenna, 135' Long for 80M and Up	**$73.99**
DXE-WA-260	Antenna, 260' Long for 160M and Up	**$89.99**

samlexamerica · ALINCO · ASTRON CORPORATION · KENWOOD · YAESU · AMERITRON

Power Supplies

Make DX Engineering your source for reliable switching and linear power supplies from major brands, including Alinco, Ameritron, Astron, Kenwood, Yaesu, and more. Choose from units with input voltages from 85 to 260 Vac and peak outputs from 10 to 50 amps.
Enter "Power Supplies" at DXEngineering.com.
Linear from $90.95; Switching from $121.95

YAESU · ICOM · KENWOOD · ALINCO · AlexLoop · GATOR Cases · STI · MASTANT ANTENNA GUYING

Request Your New DX Engineering Catalog!

Be a Better Ham! Check Out Our Blog at OnAllBands.com!

DX ENGINEERING

Ordering (via phone) Country Code: +1
9 am to midnight ET, Monday-Friday
9 am to 5 pm ET, Weekends
Phone or e-mail Tech Support: 330-572-3200
9 am to 7 pm ET, Monday-Friday
9 am to 5 pm ET, Saturday
Email: DXEngineering@DXEngineering.com

Ohio Showroom Hours:
9 am to 5 pm ET, Monday-Saturday
Ohio Curbside Pickup:
9 am to 8 pm ET, Monday-Saturday
9 am to 7 pm ET, Sunday
Nevada Curbside Pickup:
9 am to 7 pm PT, Monday-Sunday

800-777-0703 | DXEngineering.com

ON ALL BANDS · YouTube

Email Support 24/7/365 at DXEngineering@DXEngineering.com

Prices subject to change without notice. Please check DXEngineering.com for current pricing.

Aim Higher

Enter the world of SHF

IC-905

VHF/UHF/SHF All-Mode Transceiver

*Optional
CX-10G
10GHz Transverter

The IC-905 is an industry-first all-mode transceiver with 144/440/1200/2400/5600/10000* MHz coverage.

Optional Antennas

AH-24 – 2.4GHz Antenna
AH-56 – 5.6GHz Antenna
AH-100 – 10GHz Antenna
AH-109PB – 10GHz Parabolic Antenna

For the love of **ham radio.**

www.icomamerica.com/amateur
insidesales@icomamerica.com

ICOM®